

**Design and Analysis of Flywheel Energy Storage System's Structure**

by

Haizatul Hafizah Binti Hussain

Dissertation submitted in partial fulfillment of

the requirements for the

Bachelor of Engineering (Hons)

(Mechanical Engineering)

MAY 2011

Universiti Teknologi PETRONAS  
Bandar Seri Iskandar  
31750 Tronoh  
Perak Darul Ridzuan

CERTIFICATION OF APPROVAL

**Design and Analysis of Flywheel Energy Storage System's Structure**

by

Haizatul Hafizah Binti Hussain

A project dissertation submitted to the

Mechanical Engineering Programme


Universiti Teknologi PETRONAS

in partial fulfillment of the requirement for the

BACHELOR OF ENGINEERING (Hons)

(MECHANICAL ENGINEERING)

Approved by,

  
12/9/11  
\_\_\_\_\_  
(Mohd Faizairi Bin Mohd Nor)

UNIVERSITI TEKNOLOGI PETRONAS

TRONOH, PERAK

May 2011

## CERTIFICATION OF ORIGINALITY

This is to certify that I am responsible for the work submitted in this project, that the original work is my own except specified in the references and acknowledgements, and that the original work contained herein have not been undertaken or done by unspecified sources or persons.



---

HAIZATUL HAFIZAH BINTI HUSSAIN

## ABSTRACT

This dissertation, entitled “Design and Analysis of Flywheel Energy Storage System’s Structure” is to fulfill the requirement of Final Year Project II. The objectives of this project are to study and understand the principle of operation of the Flywheel Energy Storage System (FESS), to design new structure of horizontal FESS, to simulate the structural mechanics of the FESS, and to analyse static and dynamic loads on the FESS structure. FESS is a system which is targeted to be implemented and utilized as potential alternative energy in Malaysia, as the issue of oil and gas scarcity and price high is one of the major problems nowadays. The need for a clean and reliable energy from FESS is essential to reduce the green house gas emissions. FESS aims to supply uninterruptible power supply (UPS) to any system that is driven by electrical motor. The design approach of the system’s structure includes the flywheel design calculations and shaft design calculations. Detailed design is created and shaft loading analyses are executed using the Autodesk Inventor Professional Software. The results obtained from calculations are compared with the results generated by Autodesk Inventor Professional Software and ANSYS 11.0 Software. To further verify the analyses, simulations of the static and dynamic analyses are conducted using the ANSYS 11.0 Software. The final design specifications for FESS show that the most suitable material for a flywheel disc is stainless steel, with an outer diameter of 0.20 m and a shaft with 0.4 m length and 0.05 m diameter which produce 4392 rpm in its operation. The amount of kinetic energy that can be stored for a given power of 37285 W is 3.98 kJ. As one of the essential component in the FESS, the shaft design is observed to be safe to function, as it produces a negligible value of deflection and does not break during rotation. Further analysis of the electromagnetic flux induced by the system is recommended, besides generating several configurations of FESS which can give the highest efficiency to the system.

## **ACKNOWLEDGEMENTS**

I would love to convey my deepest appreciation and gratitude to everyone who has given the supports and guidance in the completion of this final year project. First and foremost, to The Creator of this universe who has given me the strength to keep on going through the challenging path of this project. I would also like to acknowledge my supervisor, Mr. Mohd Faizairi Bin Mohd Nor who has endlessly encouraged and supported me in all ways he can until the finishing point of the project. Besides that, my appreciation also goes to my colleagues from Mechanical Engineering Department who has guided me and gave valuable opinions with regard to the project. Finally, thank you very much to individuals who have directly and indirectly contributed to the success of this project. Your supports and guidance are highly appreciated.

## TABLE OF CONTENTS

<b>CERTIFICATION OF APPROVAL</b>	.	.	.	.	.	.	.	.	i
<b>CERTIFICATION OF ORIGINALITY</b>	.	.	.	.	.	.	.	.	ii
<b>ABSTRACT</b>	.	.	.	.	.	.	.	.	iii
<b>ACKNOWLEDGEMENT</b>	.	.	.	.	.	.	.	.	iv
<b>LIST OF FIGURES</b>	.	.	.	.	.	.	.	.	viii
<b>LIST OF TABLES</b>	.	.	.	.	.	.	.	.	x
<b>CHAPTER 1:</b>									
<b>INTRODUCTION</b>	.	.	.	.	.	.	.	.	1
1.1 Background	.	.	.	.	.	.	.	.	1
1.2 Problem Statement	.	.	.	.	.	.	.	.	2
1.3 Objectives and Scope of Study	.	.	.	.	.	.	.	.	2
<b>CHAPTER 2:</b>									
<b>LITERATURE REVIEW</b>	.	.	.	.	.	.	.	.	3
2.1 Principle of Operation of a Flywheel Energy Storage System	.	.	.	.	.	.	.	.	3
2.2 Types of Flywheel	.	.	.	.	.	.	.	.	4
2.2.1 Internal Combustion Engine Flywheels	.	.	.	.	.	.	.	.	4
2.2.2 Punch Press Flywheels	.	.	.	.	.	.	.	.	5
2.2.3 Solid Disk Flywheels	.	.	.	.	.	.	.	.	5
2.2.4 Composite Flywheels	.	.	.	.	.	.	.	.	6
2.3 Energy Stored in Flywheels	.	.	.	.	.	.	.	.	8
2.4 Shaft Design	.	.	.	.	.	.	.	.	9
2.5 Momentary Voltage Drop Protection Using Capacitor Self-Excited Flywheel Induction Generator	.	.	.	.	.	.	.	.	10
2.6 Japanese Flywheel Energy Storage Program	.	.	.	.	.	.	.	.	12
2.7 Uninterruptible Power Supplies (UPS)	.	.	.	.	.	.	.	.	15
2.8 Diesel Rotary UPS	.	.	.	.	.	.	.	.	16

<b>CHAPTER 3:</b>	<b>METHODOLOGY</b>	. . . . .	20
	3.1 Project Work Flow Chart	. . . . .	20
	3.2 Project Work Description	. . . . .	21
	3.3 Flywheel Design Procedure	. . . . .	21
	3.4 Shaft Design Procedure	. . . . .	22
	3.5 Detailed Design in Autodesk Inventor Professional Software	. . . . .	22
	3.6 Shaft Loading Analysis in Autodesk Inventor Professional Software	. . . . .	22
	3.7 Static and Dynamic Analyses in ANSYS 11.0 Software	. . . . .	23
<b>CHAPTER 4:</b>	<b>RESULTS AND DISCUSSION</b>	. . . . .	24
	4.1 Schematic Diagram	. . . . .	24
	4.2 Flywheel Design Calculation	. . . . .	24
	4.2.1 Preliminary Calculation for Material Selection		24
	4.2.2 Mass Moment of Inertia	. . . . .	25
	4.2.3 Burst Speed	. . . . .	26
	4.2.4 Amount of Energy Required	. . . . .	26
	4.2.5 Flywheel Geometry	. . . . .	27
	4.2.6 Stresses in Flywheel	. . . . .	27
	4.3 Shaft Design Calculation	. . . . .	30
	4.3.1 Torsion Moment	. . . . .	30
	4.3.2 Free Body Diagram	. . . . .	30
	4.3.3 Shaft Loading	. . . . .	31
	4.4 Detailed Design	. . . . .	39
	4.5 Static and Dynamic Analyses.	. . . . .	40
	4.6 Final Design Specifications	. . . . .	43
	4.6.1 Final Design Geometry	. . . . .	43

4.6.2 Flywheel Disc	.	.	.	.	.	.	.	44
4.6.3 Shaft	.	.	.	.	.	.	.	45
<b>CHAPTER 5:</b>								
<b>CONCLUSIONS AND RECOMMENDATIONS</b>								47
<b>REFERENCES</b>	.	.	.	.	.	.	.	48
<b>APPENDICES</b>	.	.	.	.	.	.	.	50



## LIST OF FIGURES

Figure 2.1	Turning moment diagram for a four stroke internal combustion engine	4
Figure 2.2	Punch press cycle – torque versus time	5
Figure 2.3	Solid disk flywheel on a rotating shaft	6
Figure 2.4	Composite Flywheel	7
Figure 2.5	Composite Flywheel Dimensions	7
Figure 2.6	Flywheel with arms	9
Figure 2.7	Whole system of momentary voltage drop protection using self-excited induction generator	11
Figure 2.8	Photo of the induction motor with flywheel and capacitors	11
Figure 2.9	The concept of daily load leveling by electric power storage system (New Energy and Industrial Technology Development Organization (NEDO))	12
Figure 2.10	Flywheel system and details of superconducting magnetic bearing assembly	14
Figure 2.11	Operation of the magnetic bearing (New Energy and Industrial Technology Development Organization (NEDO))	14
Figure 2.12	Whole System of the Flywheel UPS (Nippon Flywheel Corporation)	16
Figure 2.13	Basic Principle Diagram	18
Figure 2.14	Basic Schematic Diagram of a Diesel Rotary UPS	19
Figure 3.1	Project Work Flow Chart	20
Figure 4.1	Schematic Diagram of FESS Structure	24

Figure 4.2	Flywheel Geometry	27
Figure 4.3	Free Body Diagram of FESS	30
Figure 4.4	Applied loads and supports on shaft	35
Figure 4.5	Applied loads and supports on shaft in 3D view	35
Figure 4.6	Shear Force Diagram	36
Figure 4.7	Bending Moment Diagram	36
Figure 4.8	Bending Stress Diagram	37
Figure 4.9	Deflection Angle Diagram	38
Figure 4.10	Deflection Diagram	38
Figure 4.11	Detailed Design of Flywheel Energy Storage System Structure	39
Figure 4.12	Geometry and Meshing of FESS	40
Figure 4.13	Total Deformation	40
Figure 4.14	Maximum Principal Stress	41
Figure 4.15	Maximum Shear Stress	41
Figure 4.16	Strain Energy	42
Figure 4.17	Total Acceleration	42
Figure 4.18	Final design in 3D view	43
Figure 4.19	Base view and projected views of final design	43

## **LIST OF TABLES**

Table 4.1	Calculation of torque of the possible materials of flywheel	25
Table 4.2	Summary of stresses in flywheel	29
Table 4.3	Design's parts' list	39
Table 4.4	Flywheel Disc Specifications	44
Table 4.5	Shaft Forces and Reaction Supports	45
Table 4.6	Shaft Loadings on Driver and Flywheel Disc	45

# CHAPTER 1

## INTRODUCTION

### 1.1 Background

This project is focused on designing and analysing the flywheel energy storage system's (FESS) structure. Flywheels have been used to smooth out the rotation of steam engines and internal combustion engines, where in both cases the pulsed input energy is stored as rotational kinetic energy in the flywheel. The FESS is also concerned on the uninterruptible power supplies (UPS). The request in the continuous power supply has been a great demand in today's world, as communications which usually use electrical devices is widely used by everyone in the world. Therefore, UPS are installed in factories, hospitals, offices, and many other places. Pb-Acid battery system is one of the most common UPS that utilizes power electronic devices to convert voltage and frequency.

Flywheels are also being used in hybrid vehicles in the regenerative braking energy. It is an energy recovery mechanism which slows down a vehicle by converting its kinetic energy into other form which can later be used immediately or stored for future use. Since a flywheel is used to smooth out the rotation of an internal combustion engine in a vehicle, the amount of energy stored is quite small and is limited by the need for the engine to be able to accelerate reasonably quickly when required. The design of the flywheel and the method used to transfer energy in and out must be optimized so that a significant amount of energy can be stored.

## **1.2 Problem Statement**

The need for green technology applications from FESS is essential to reduce the greenhouse gas emissions. Due to the issue of oil and gas scarcity and price high, researchers are looking into reliable alternative energy. One possible alternative energy source is flywheel which concerns on the UPS. The current UPS system is not widely being used for constant resource of continuous energy. The UPS with flywheel design is still new and needs further researches to be used as possible power sources in the future. The need for clean, reliable and perpetual energy is also the aim for this project.

## **1.3 Objectives and Scope of Study**

The objectives of this project are as follows:

- To study and understand the principle of operation of the FESS.
- To design new structure of horizontal FESS.
- To simulate the structural mechanics of the FESS based on the loads applied.
- To analyse static and dynamic loads on the FESS structure.

The scope of work for FYP I is to do research and understand the FESS, which comprises of the background, the principle of operation, literature reviews, and the energy equations related. Design concepts are created using Autodesk Inventor Professional Software. Following that, the scope of work for FYP II is to continue on the flywheel design calculation and shaft design calculation. Detailed design, static analysis, dynamic analysis, and structural mechanics simulations of the FESS structure using Autodesk Inventor Professional Software and ANSYS 11.0 Software are conducted to validate the results obtained from calculations. Lastly, the final design specifications of FESS are specified.

## CHAPTER 2

### LITERATURE REVIEW

#### 2.1 Principle of Operation of a Flywheel Energy Storage System

Flywheel is essentially a simple device for storing energy in a rotating mass has been known for centuries (Ashley, 1993). It is only since the development of high-strength materials and magnetic bearings (DeTersa, 1999) that this technology is gaining a lot more attention. Using magnetic bearings make it possible to reach high operating speeds providing cleaner, faster and more efficient bearing equipment at extreme temperatures. Recently designed flywheels could offer orders of magnitude increases in both performance and service life (Sung Kyu et al., 2001; Moritz B., 1998; George et al., 2000), in addition, large control torques and momentum storage capability for spacecraft, launch vehicles, aircraft power systems and power supplies (Anerdi et al., 1994; Christopher et al., 1998; Rodriguez et al., 1983).

The flywheel system mainly consists of flywheel rotor, motor/generator, magnetic bearings, housing and power transformation electronic system (Kojima et al., 1997). In the development of the flywheel, current researches focused on increasing the performance while meeting the safety considerations. The kinetic energy stored in a rotating mass is given as:

$$E_k = \frac{1}{2} I\omega^2 \text{ [J]} \quad (1)$$

Where  $I$  is the mass moment of inertia and  $\omega$  is the angular velocity. Mass moment of inertia can be obtained by the mass and geometry of the flywheel and given as:

$$I = \int x^2 dm_x \text{ [kgm}^2\text{]} \quad (2)$$

Where  $x$  is the distance from rotational axis to the difference mass  $dm_x$ . For solid cylindrical disk,  $I$  is given as:

$$I = \frac{1}{2} mr^2 \quad (3)$$

Where  $m$  is the mass and  $r$  is the radius of the flywheel.

The FESS operates by accelerating the rotor (flywheel) to a very high speed and maintaining the energy in the form of rotational energy. The flywheel's rotational energy is reduced when energy is extracted from the system. Most of them use electricity to operate and research on using mechanical energy is currently being developed.

## 2.2 Types of Flywheel

### 2.2.1 Internal Combustion Engine Flywheels

Referring to Figure 2.1, the energy is developed during one stroke and the engine is to run for the whole cycle, utilizing the energy stored during the first stroke. For instance, for a four stroke internal combustion engine, energy is developed during the power stroke, which will eventually supply it back to the engine during the suction, compression, and exhaust stroke. The energy will be absorbed by the flywheel to be transferred to the crankshaft for rotational motion at constant speed. When the flywheel absorbs energy, its speed increases, however when it releases energy, its speed decreases. Therefore, a flywheel does not maintain constant speed. It simply reduces the fluctuation of speed of the engine.

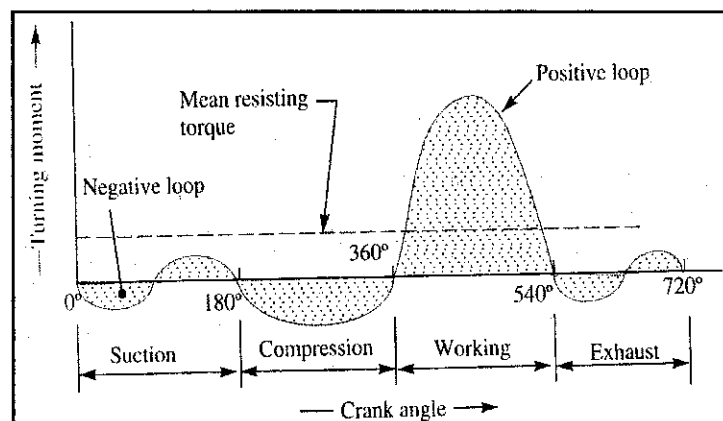


Figure 2.1: Turning moment diagram for a four stroke internal combustion engine  
(Juvinall, R. C., Marshek, K. M., 1991)

### 2.2.2 Punch Press Flywheels

A punch press operates cyclically to stamp out parts or punch holes in parts. The inertial energy of the system which is contained in an appropriately designed flywheel does the actual punching. The electric motor that is connected to the punch press is then used to return the flywheel to its initial punching speed before the next punching cycle begins. Based on Figure 2.2, the time  $t_1$  is the length of the actual punching process and time  $t_2$  is the start of the next cycle. During the time interval,  $t_2 - t_1$ , the system must recover.

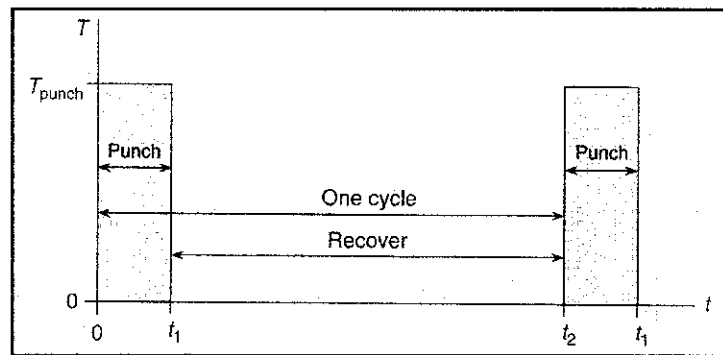


Figure 2.2: Punch press cycle – torque versus time  
(Juvinall, R. C., Marshek, K. M., 1991)

### 2.2.3 Solid Disk Flywheels

Figure 2.3 shows a solid disk flywheel with shaft in the middle supported by appropriate bearings at each end. The applied torque,  $T$  produces an angular acceleration,  $\alpha$ , which in turn produces an angular velocity,  $\omega$ . The torque,  $T$  can vary over time; therefore the angular acceleration,  $\alpha$ , and angular velocity,  $\omega$  must also vary over time.

$$T = I_{total} \alpha = (I_{flywheel} + I_{shaft}) \alpha \quad (4)$$

Where  $I_{total}$  is the total mass moment of inertia, which is the sum of the mass moment of inertia of the flywheel ( $I_{flywheel}$ ) and the mass moment of inertia of the shaft ( $I_{shaft}$ ), both calculated about the axis of rotation.



For a solid disk flywheel with an outside radius ( $r_o$ ) and inside radius ( $r_i$ ) mounted on a shaft with an outside radius equal to the inside radius of the flywheel, the mass moments of inertia ( $I_{flywheel}$ ) and  $I_{shaft}$  are given by:

$$I_{flywheel} = \frac{1}{2} \rho \pi t (r_o^2 - r_i^2)^2 \quad (5)$$

$$I_{shaft} = \frac{1}{2} \rho \pi L r_i^4 \quad (6)$$

Where  $t$  is the thickness of the flywheel and  $L$  is the length of the shaft, and the density,  $\rho$  of the flywheel and shaft are assumed to be the same.

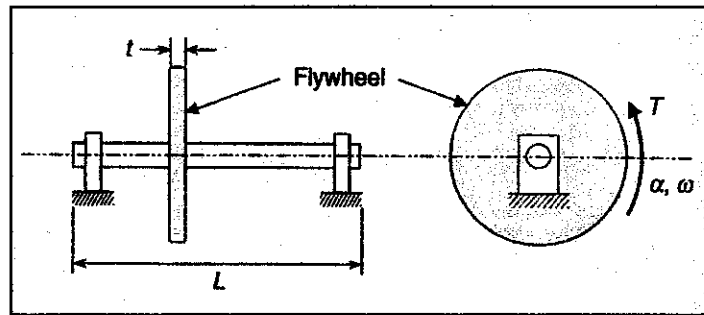


Figure 2.3: Solid disk flywheel on a rotating shaft  
(Juvinall, R. C., Marshek, K. M., 1991)

## 2.2.4 Composite Flywheels

The composite flywheel, as in Figure 2.4 is the simplest design, which is a solid circular disc. Although this is probably the easiest and most economical design to produce, it is not the most efficient use of material, which is weight. In fact, better design can be achieved by moving material from location near the axis of rotation to a farther location from the axis. This is because the mass moment of inertia is a measure of the distribution of mass. Mass located farther away from the axis counts more than the same amount of mass located near the axis. Figure 2.5 shows the composite flywheel dimensions, which consists of an inner hub, an outer rim, and spokes which connect the hub with rim. The total mass moment of inertia can be determined by adding up each component's mass moment of inertia.

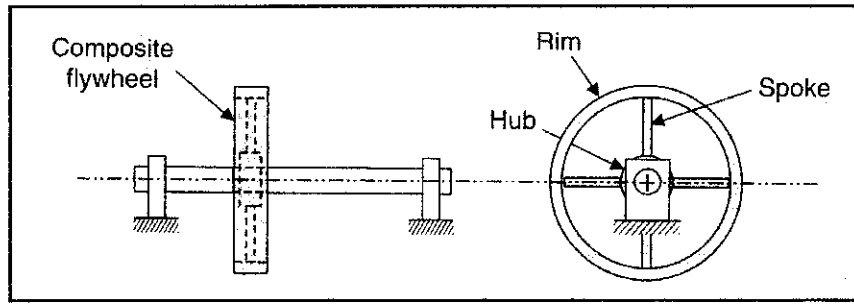


Figure 2.4: Composite Flywheel (Juvinall, R. C., Marshek, K. M., 1991)

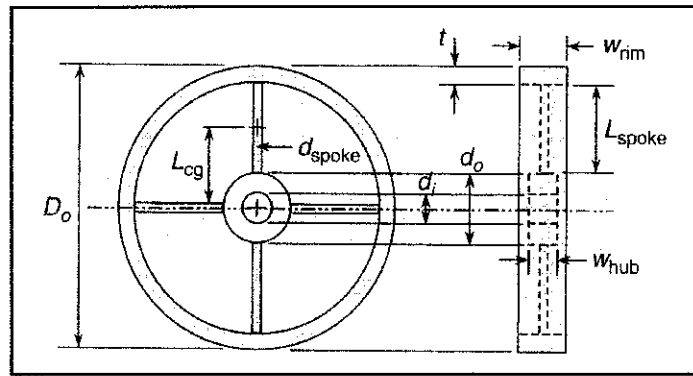


Figure 2.5: Composite Flywheel Dimensions (Juvinall, R. C., Marshek, K. M., 1991)

Mass moment of inertia of hub

$$I_{hub} = \frac{1}{2} m_{hub} (r_o^2 - r_i^2) = \frac{1}{8} m_{hub} (d_o^2 - d_i^2) \quad (7)$$

Mass of the hub is given by:

$$m_{hub} = \rho \pi w_{hub} (r_o^2 - r_i^2) = \frac{1}{4} \rho \pi w_{hub} (d_o^2 - d_i^2) \quad (8)$$

Mass moment of inertia of rim

$$I_{rim} = m_{rim} r_o^2 = \frac{1}{4} m_{rim} d_o^2 \quad (9)$$

Mass of the rim is given by:

$$m_{rim} = 2 \rho \pi r_o t w_{rim} = \rho \pi d_o t w_{rim} \quad (10)$$

### Mass moment of inertia of spoke

$$I_{spoke} = m_{spoke}(1/12 L_{spoke}^2 + L_{cg}^2) \quad (11)$$

Mass of the spoke is given by:

$$m_{spoke} = \rho \pi L_{spoke} r_{spoke}^2 = 1/4 \rho \pi L_{spoke} d_{spoke}^2 \quad (12)$$

$$\text{Total mass moment of inertia, } I_{flywheel} = I_{hub} + I_{rim} + N_{spokes} I_{spoke} \quad (13)$$

### **2.3 Energy Stored in Flywheel**

The energy stored in flywheel based on Figure 2.6 is  $\Delta E = m.R^2.\omega^2.C_S = m.v^2.C_S$ . The derivation of the equation is as attached in Appendix I.

From this equation, the mass of the flywheel rim may be determined. However,

- Only the mass moment of inertia of the rim is considered, whereas the mass moment of inertia of the hub and arms is neglected. This is because the major portion of weight of the flywheel is in the rim and a small portion in the hub and arms. Furthermore, the hub and arms are located nearer to the axis of rotation, which makes them less significant, in terms of their mass moment of inertia.
- The mass of the flywheel is:  $m = \text{volume} \times \text{density}$
- The cross-sectional area of the rim is:  $A = b \times t$  (assuming the rim to be rectangular)

Where  $b = \text{width of the rim}$

$t = \text{thickness of the rim}$

The maximum kinetic energy that can be stored in a particular flywheel is determined by the density and the tensile strength of the material chosen to build the flywheel.

$$\text{Energy density} = E/m = k(\sigma/\rho) \quad (14)$$

where  $\sigma$  is the tensile strength of the flywheel material,  $\rho$  is the density of the flywheel, and  $k$  is a constant depending on the geometry or shape of the flywheel disc ( $k$  is 0.5 for a thin rim disc; 0.6 for a flat disc; and 0.8 for a truncated conical disc designed to obtain equal stress throughout the flywheel and therefore maximum energy storage density).

Therefore, to obtain a high-energy density of flywheel, the material used must be of light weight with high tensile strength.

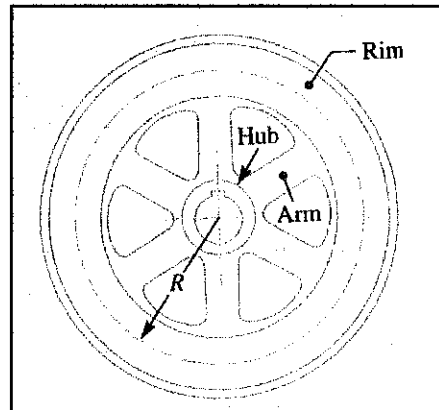


Figure 2.6: Flywheel with arms (Juvinall, R. C., Marshek, K. M., 1991)

## 2.4 Shaft Design

In shaft design, the typical issues that are taken into consideration are: loads, materials, environment, vibration, and deflections. Shaft power can be defined as the time rate of change of energy or better known as work.

$$\text{Power} = \text{Torque} \times \text{Angular Velocity} \quad (15)$$

Shaft stresses which are bending stress and torsional shear stress can be calculated as below:

Bending Stress: 
$$\sigma_{alt} = k_f \frac{M_a c}{I} \quad (16)$$

$$\sigma_{mean} = k_{fm} \frac{M_m c}{I} \quad (17)$$

Torsional Shear Stress: 
$$\tau_{alt} = k_{fs} \frac{T_a r}{J} \quad (18)$$

$$\tau_{mean} = k_{fsm} \frac{T_m r}{J} \quad (19)$$

The three common types of vibration that are encountered by shafts are lateral vibration, shaft whirl, and torsional vibration. In connecting one shaft to another, couplings are used to accommodate the misalignment that occurs.

## **2.5 Momentary Voltage Drop Protection Using Capacitor Self-Excited Flywheel Induction Generator**

One of the simplest devices to protect from just 0.1 s voltage drop in electrical devices is by using capacitor self-excited induction generator. An electromagnetic force is induced in the machine windings due to the excitation by capacitor when an appropriate three-phase capacitor bank is connected across an induction motor. This is called as capacitor self-excitation, which can be utilized as generator to run the induction machine. Figure 2.7 shows the whole system of momentary voltage drop protection using capacitor self-excited flywheel induction generator.

In normal conditions, motor is driven by a power source that sets parallel with specific load. When voltage drop occurs and volt-meter detects the latter, switch-A (SW.A) immediately turns off to protect from reverse power. The self-excited induction motor becomes generator and eventually supplies power to load. As it supplies power, angular velocity decreases, indicating that the output voltage and frequency decays. After the line voltage recovers, SW.A turns on immediately while SW.B turns off. One of the principles of this system is that momentary voltage drop protector supplies frequency and voltage to the specific load which decrease gradually. Nevertheless, some electronic devices are not affected by a little fluctuation of line frequency and voltage because AC/DC converters are embedded in them. Figure 2.8 shows the photo of the induction motor with flywheel and capacitors.

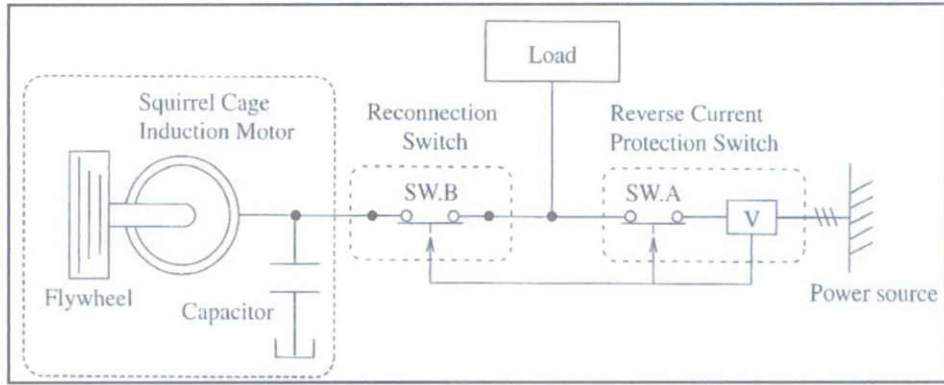


Figure 2.7: Whole system of momentary voltage drop protection using self-excited induction generator (Kojima A, et al. (1997))

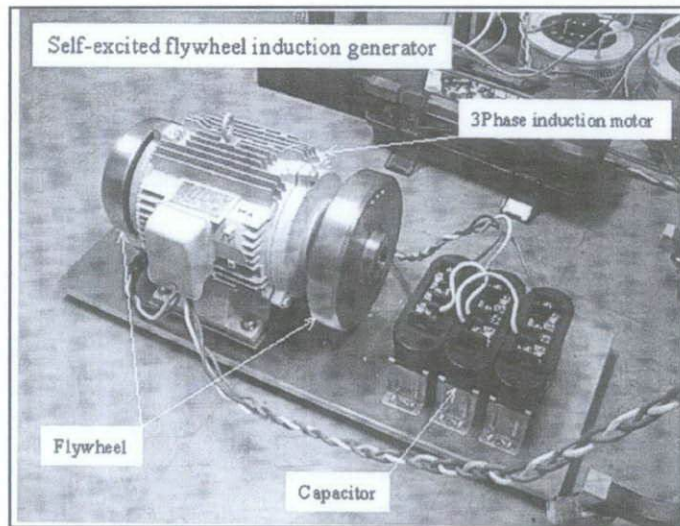


Figure 2.8: Photo of the induction motor with flywheel and capacitors (Kojima A, et al. 1997)

## 2.6 Japanese Flywheel Energy Storage Program

In Japan, the demand for power is increasing more rapidly than in the United States. Diurnal or daily load leveling is the most desirable solution, to have a mechanism in storing power at night and feeding it back to the consumers into the grid during the day. To cater with this problem, two programs are actively practiced in Japan, which are the superconducting magnetic energy storage (SMES) program and the superconducting flywheel energy storage, which focus on diurnal load leveling. Figure 2.9 shows the concept of daily load leveling by electric power storage system.

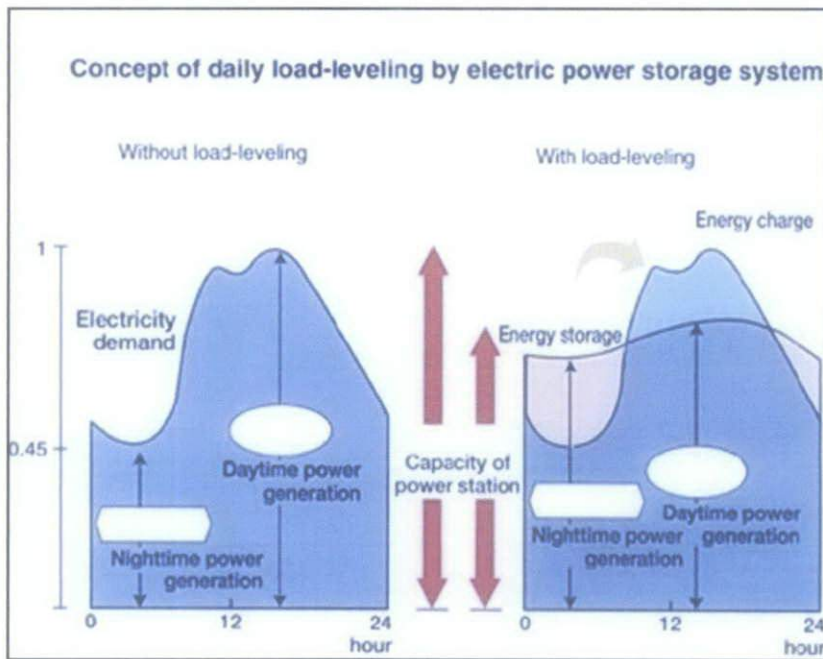


Figure 2.9: The concept of daily load leveling by electric power storage system (New Energy and Industrial Technology Development Organization (NEDO) n.d)

Typically commercialized flywheels are made of metal. To maintain the tensile stresses in the flywheel within reasonable limits, it rotates at relatively low speeds. However, by increasing rotational speed, it will yield to a large benefit in energy density. Therefore, today's flywheels consider using fiber-reinforced plastics (FRP) instead of metal, which can be engineered to have very high strength in the radial direction, consequently can produce higher operational speeds. Furthermore, they can also be designed to fracture

into small pieces in case of structural failure. An additional advantage of using FRP as the material for flywheel is that, the lighter flywheel simplifies the design of magnetic bearing.

Loss in the bearings is the factor that reduces the efficiency of flywheel in the long-term basis of energy storage. This is because, any mechanical bearing which have direct contact between the stationary and rotating parts will have enough loss to render the system uneconomical (Higasa, 1994). To overcome this problem, non-contact active magnetic bearing that employs conventional electromagnets is used. Under the same condition, the rotational loss is 1-10% that of a mechanical bearing.

However, the bearing itself consumes power which is dissipated as heat in the copper electromagnets. The bearing and cooling system power consumption must be included in the calculation of the overall system efficiency. Superconducting magnetic bearings have shown losses of  $10^{-2}$  to  $10^{-3}$  watts per kg for a 2000 rpm rotor, which indicates to an overall one-day or “round trip” system efficiency of 84% which is acceptable.

Figure 2.10 and 2.11 show the basic operation of the bearing and flywheel. The flywheel, at room temperature, carries a permanent ring magnet on its lower surface, which rides above the superconducting portion of the bearing, consists of an array of pellets of yttrium-barium-copper-oxide, YBCO. The YBCO traps the magnetic flux which is produced by the permanent magnet. As long as the pinning force of the YBCO is not exceeded, the bearing generates restoring forces in order to counter any relative motion of the superconductor and permanent magnet. Therefore, the bearing is completely passive and does not require any complex feedback and control circuits needed for conventional magnetic bearings.



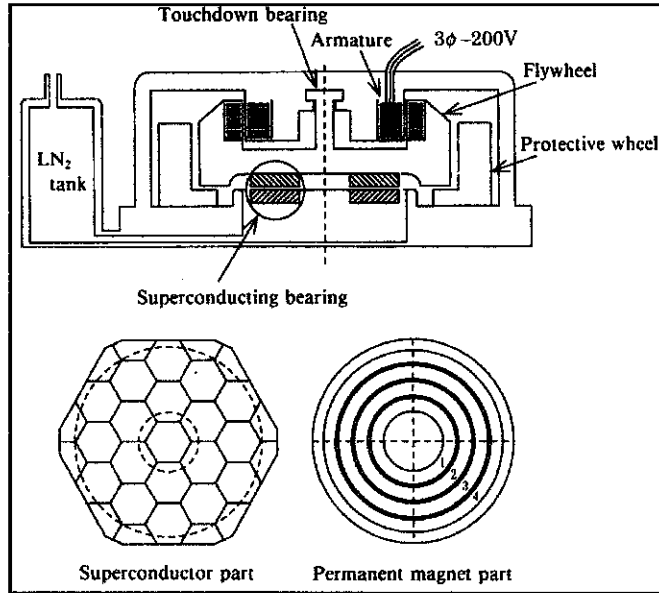


Figure 2.10: Flywheel system and details of superconducting magnetic bearing assembly (Higasa 1994)

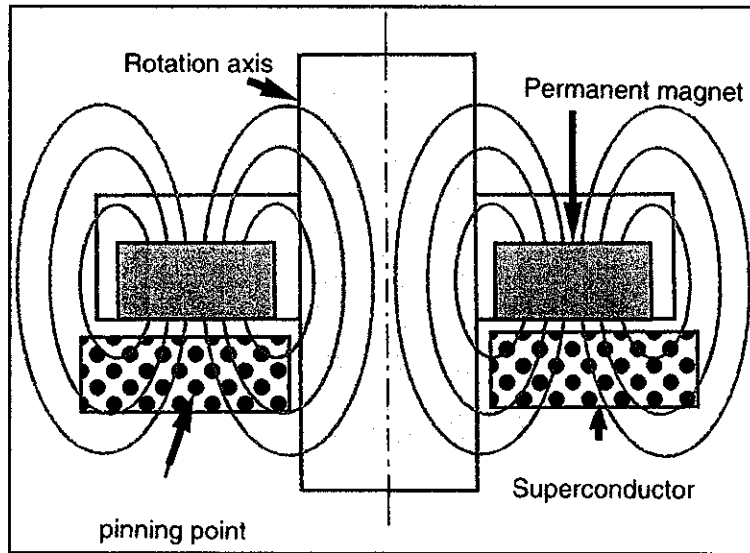


Figure 2.11: Operation of the magnetic bearing (New Energy and Industrial Technology Development Organization (NEDO) n.d)

## 2.7 Uninterruptible Power Supplies (UPS)

Flywheel stores the kinetic energy mechanically. The most important component of a flywheel is the mass which stores the energy have shapes such as rings, disks, or discrete weights. The kinetic energy stored in the rotor of flywheel is directly proportional to the rotor mass and to the square of its angular velocity. By converting the kinetic energy (rotating) to electric by motor or generator machine, electricity can be stored. Nippon Flywheel Corporation is one of the manufacturers that produce flywheel UPS. However, the flywheel is quite conventional since it is using low angular velocity iron casting rotor which can only compensate within the range of 5kV A-10 s of power failure.

In normal condition, the input power goes through inverter-1 and LC filter, then only supplies to the specific load in a form of sine wave. The term storing energy means to keep the flywheel angular velocity and power flows to the flywheel through the inverter-2 as shown in Figure 2.12. Therefore, when shutdown or momentary voltage drop happens, flywheel energy is discharged through both inverters to the specific load. As a result, UPS can supply constant frequency and voltage to the specific load continuously.

In the energy storage system where the flywheel system is installed, the flywheel must be rotating continuously to overcome its mechanical loss that is contributed by windage loss and bearing loss. The kinetic energy also must be converted to electricity by means of power electronics devices like inverters which cause idling energy loss and conversion loss. Basically, the mechanical loss is greater than that of electric. Hence, if the mechanical loss can be minimized, total flywheel efficiency can be improved effectively. To achieve that, rotor is driven in vacuum condition by using superconductive magnet bearing and so on.

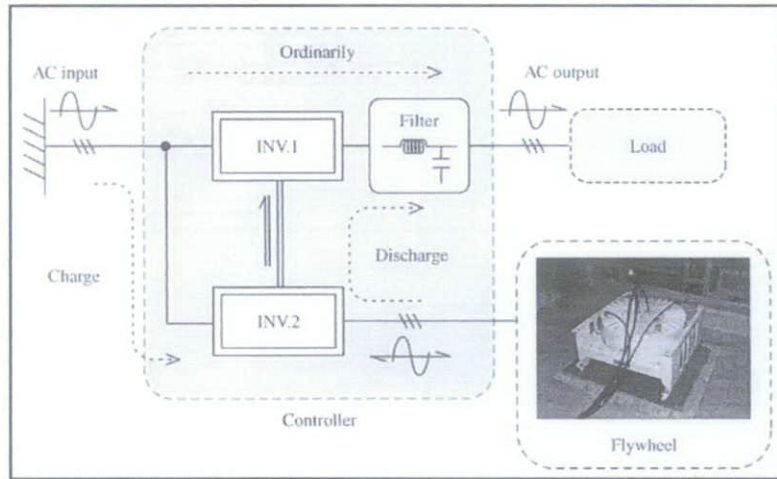


Figure 2.12: Whole System of the Flywheel UPS (Nippon Flywheel Corporation)  
(Kojima A, et al. 1997)

## 2.8 Diesel Rotary UPS

Generally, most types of UPS which are battery-powered are used if the main electricity fails can only store a small amount of energy, which lasts for a few minutes only. A diesel-generator back-up system is then needed to get a UPS. A Diesel Rotary UPS (DRUPS) device combines the function of a battery-powered UPS and diesel-generator, as shown in Figure 2.13. An electrical generator which functions as motor stores the kinetic energy in an electro-mechanical flywheel. It also functions as active filter for all sorts of power quality problems, such as frequency variations, harmonics, and others.

When the main electricity supply fails, the stored energy in flywheel is released to drive the electrical generator, which will then supply power to the load without any interruption. At the same time, the diesel is started up and after approximately two to three seconds, the diesel engine takes over from the flywheel to drive the electrical generator to create the electricity. Typically, a DRUPS has enough fuel to power the load for days and also weeks if the main electricity supply fails. The advantages of DRUPS device are higher energy efficiency, smaller footprint, less components usage, longer technical lifetime, and no chemical waste.

A DRUPS device uses the effect of inertia of a high-mass spinning flywheel to provide a short-term energy supply in case of power loss. Moreover, the flywheel acts as a buffer against power spikes and sags, since such short-term power events are not able to affect the rotational speed of the high-mass flywheel. This type of UPS can be considered as on-line since it spins continuously under normal conditions. Compared to a battery-based UPS, flywheel-based UPS system typically provides 10 to 20 seconds of protection before the flywheel slowed down and the power output stops. It is usually used together with the standby diesel-generators, which provide backup power only for a short period of time where the engine needs to start running and stabilize its output. Basically, larger flywheel or multiple flywheels which operates in parallel can increase the reserve running time or capacity.

Since the flywheel is the mechanical power source, it does not necessarily use an electric motor or generator as an intermediate between it and a diesel engine. To start up a diesel engine, the rotational inertia of the flywheel can be used to directly spin the flywheel by using a transmission gearbox. Then, once the flywheel is running, the diesel engine can be used to directly spin the flywheel. In case of using multiple flywheels, they can be connected in parallel through mechanical countershafts.

Generally, a DRUPS is designed to provide a very high current output compared to a purely electronic UPS. It is also better in providing inrush current for inductive loads such as motor startup or compressor loads. Besides that, it is able to tolerate short-circuit conditions up to 17 times larger than an electric UPS, where it permits one device to fail while letting other devices to still operate by the power supply from the DRUPS. The life cycle of a DRUPS is longer than that of a purely electronic UPS by 30 years or more. However, they require a periodic downtime for mechanical maintenance such as ball bearing replacement. To increase standby efficiency and reduce the maintenance requirements, magnetic bearings and air-evacuated enclosures are used in the newer rotary units.

Basically, the high-mass flywheel is used together with a motor-generator system and can be configured as follows:



1. A motor driving a generator which is connected mechanically;
2. A combined synchronous motor and generator wound in the alternating slots of a single stator and rotor;
3. A hybrid rotary UPS which is designed similar to an online UPS, except that it uses the flywheel instead of batteries. The rectifier drives a motor to rotate the flywheel while a generator uses the flywheel to power up the inverter.

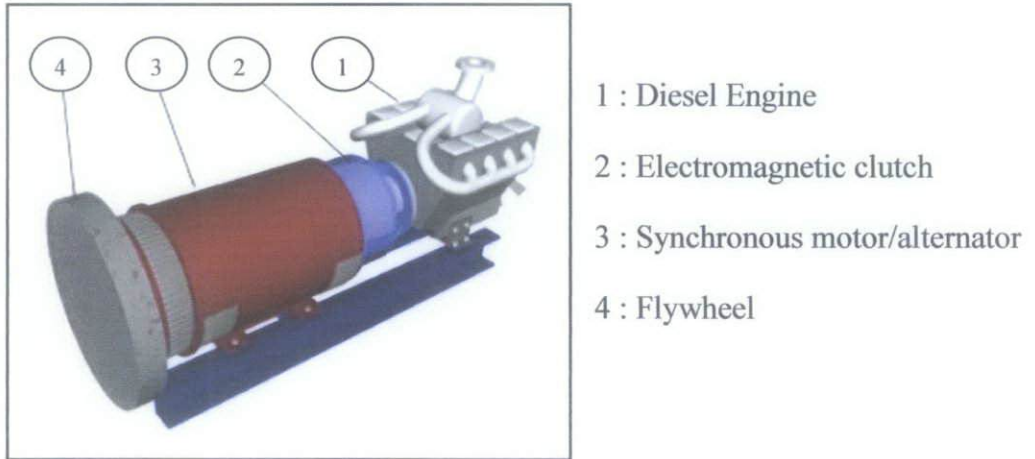


Figure 2.13: Basic Principle Diagram (Hitzinger, 2001)

Figure 2.14 shows the basic schematic diagram of a diesel rotary UPS. Some DRUPS systems consists of an AC Motor Generator (M-G) set with a flywheel, as well as storage batteries, inverter, rectifier, static switch and solid state circuitry. The M-G set and the rectifier/storage batteries/inverter combination represent parallel supply paths, and either path is capable of supplying the load. During normal operation, the M-G set powers the computer loads while the off-line static section, which is on stand-by mode charges the system batteries.

During the event of power loss in the utility feed, the control circuitry will disconnect the M-G set from the utility by opening the static switch and closing the inverter-output circuit breakers, which then allows the system batteries to power the M-G set through the inverter. The mechanical energy which is stored in the flywheel allows the M-G set to continue to deliver its full-rated output for a minimum of 200 milliseconds. This gives

the control system time to detect a loss of power supply and transfer the loads' supply to the battery/inverter combination.

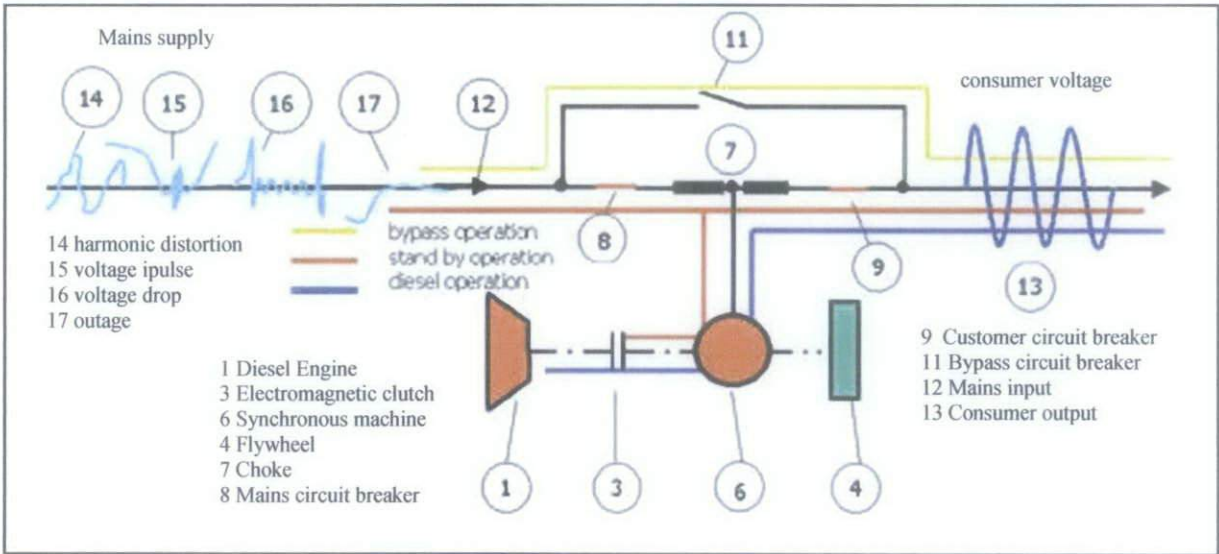


Figure 2.14: Basic Schematic Diagram of a Diesel Rotary UPS (Hitzinger, 2001)

# CHAPTER 3

## METHODOLOGY

### 3.1 Project Work Flow Chart

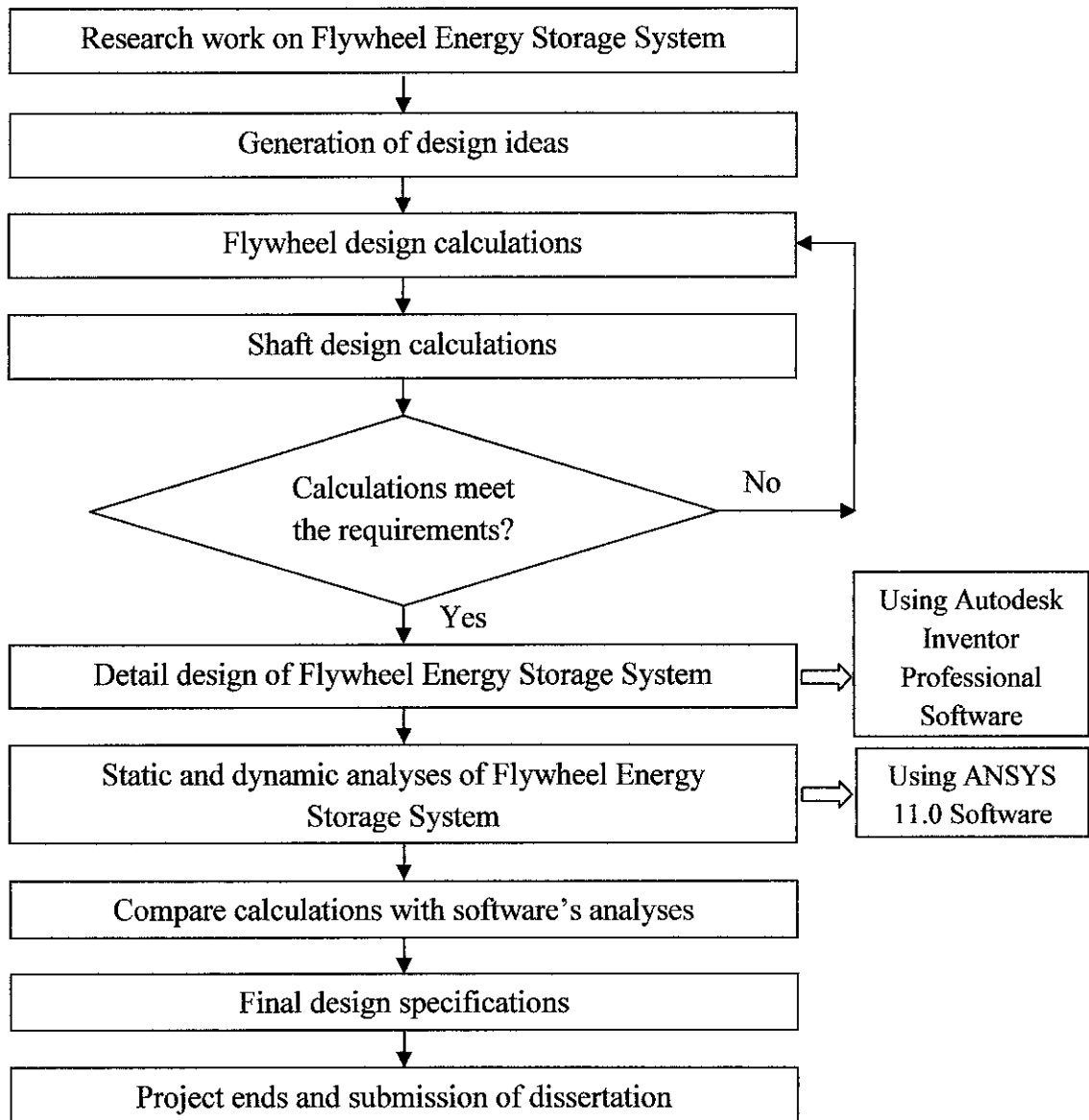


Figure 3.1: Project Work Flow Chart

### **3.2 Project Work Description**

Based on the project work flow chart, it can be divided into three main phases:

1. Understanding the project;
2. Design of FESS;
3. Analysis of FESS.

In understanding the project phase, research works are done to familiarize on what FESS is all about, which comprises of its principle of operation, the basic equations and terms related, the related literature reviews, the materials used, and its recent applications.

Moving on to the design of FESS phase, there are two main stages involved which are planning and executing. In the planning stage, research work on the current design of flywheel is done to obtain a clearer view on how to proceed with the generation of design ideas. Next, the executing stage includes creating conceptual design of flywheel and its components, flywheel design calculations and shaft design calculations. If the calculations meet the standard requirement, further analysis can proceed, such as the detail design of FESS and shaft loading analysis using the Autodesk Inventor Professional Software.

Lastly, in the analysis of FESS phase, static analysis, dynamic analysis, and simulations are executed using ANSYS 11.0 Software. The results are compared with the previous calculations and further data interpretation and discussions follow. Finally, the final design specifications are decided.

### **3.3 Flywheel Design Procedure**

1. Select material based on the preliminary calculations of torque produced.
2. Determine the mass moment of inertia of flywheel.
3. Calculate the burst speed of flywheel.
4. Calculate the energy stored in the flywheel.
5. Define flywheel geometry: solid disc or flywheel with spokes.
6. Determine the stresses associated with the flywheel.



### **3.4 Shaft Design Procedure**

1. Determine the torque on the shaft for a given input power.
2. Draw a free body diagram and model the various machine elements mounted on the shaft, in terms of forces and torques.
3. Calculate the shaft loadings which act on desired locations, such as on the driver, flywheel disc and the cylindrical roller bearings on both shaft's ends.
4. Develop the shear and moment diagrams of the shaft. Identify the bending moment which causes normal stress and torque which causes shear stress.
5. Compare the calculated values with the values generated by the software.

### **3.5 Detailed Design in Autodesk Inventor Professional Software**

1. Create new parts in the standard (mm) .ipt template, in the 2D sketch blocks. The parts are: flywheel disc, driver, and magnet.
2. Insert dimensions during sketching to control the size intended.
3. Extrude those parts to convert it into 3D image components.
4. Open up the Assembly Files in the standard (mm) .iam template to place all the components sketched together as a single functional unit. Flywheel disc and magnets are assembled together, as well as driver and magnets; before they are assembled further with the other components.
5. Choose cylindrical roller bearings (SKF Series CRM – SKF CRM 11A) at the Content Center Parts to be attached at both ends of the shaft.
6. Select shaft with appropriate length and diameter.
7. Create a drawing of the assembly by using Drawing Files.

### **3.6 Shaft Loading Analysis in Autodesk Inventor Professional Software**

1. Open up the Shaft Component Generator after the assembly of all parts of FESS.
2. Apply appropriate reaction forces, radial forces, moment, torque, and supports on desired locations.
3. Click 'calculate' and graphs' selections appears.

### 3.7 Static and Dynamic Analyses in ANSYS 11.0 Software

1. Import assembly drawing from Autodesk Inventor Professional Software into ANSYS 11.0 Software.
2. Assign materials of each parts of the assembly which are;
  - Flywheel : Stainless Steel
  - Magnets : Cast Iron
  - Shaft : Stainless Steel
  - Driver : Stainless Steel
3. Generate mesh on the assembly.
4. Select static structural option in new analysis,
5. Apply fixed support on both shaft's ends and bearings.
6. Apply frictionless support along the shaft.
7. Apply force on the flywheel disc,  $F = 3450 \text{ N}$ ; and on the driver,  $F = 4929 \text{ N}$ .
8. Apply pressure along the flywheel disc,  $P = 36606 \text{ Pa}$  and on the driver,  $P = 52298 \text{ Pa}$ .
9. Apply moment of  $81.06 \text{ N.m}$  on shafts in clockwise direction.
10. Apply rotational velocity of  $459.96 \text{ rad/s}$  on shaft in clockwise direction.
11. Select flexible dynamic analysis option for dynamic analysis and repeat step 5 to 10.
12. Solve all results for deformation, strain, and stress solutions.

*Note: For items No. 7 until 10, the values are obtained from the calculations provided in the later chapter, prior to the static and dynamic analyses.*

## CHAPTER 4

### RESULTS AND DISCUSSION

#### 4.1 Schematic Diagram

Based on Figure 4.1, the magnets are attached to the flywheel itself, thus act as generator to store energy as well as to supply energy to the driver. There are three possible materials that can be used as flywheel, which are cast iron, stainless steel, and aluminium. The material selection is discussed further in the later subtopic.

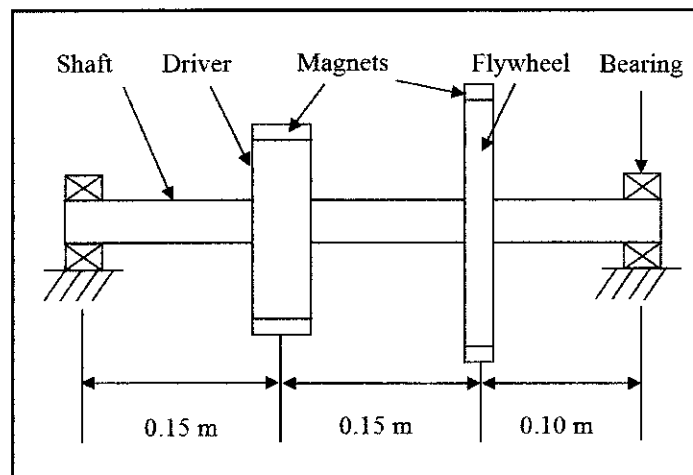


Figure 4.1: Schematic Diagram of FESS Structure

#### 4.2 Flywheel Design Calculation

##### 4.2.1 Preliminary Calculation for Material Selection

$$T = I_{total} \alpha = (I_{flywheel} + I_{shaft}) \alpha$$

$$I_{flywheel} = \frac{1}{2} \rho \pi t (r_o^2 - r_i^2)^2$$

$$I_{shaft} = \frac{1}{2} \rho \pi L r_i^4$$

Table 4.1 shows the calculation of torque of the possible materials of flywheel. The full calculation of  $I_{flywheel}$ ,  $I_{shaft}$ , and torque,  $T$  can be referred to **Appendix 2**. From this preliminary calculation for material selection, the torque produced when using stainless steel flywheel is larger compared to the torque produced by cast iron flywheel and aluminium flywheel.

$$T_{\text{stainless steel}} > T_{\text{cast iron}} > T_{\text{aluminium}}$$

This is because aluminium has the lowest density, compared to the cast iron and stainless steel. Therefore, it produces the smallest magnitude of torque when all the other parameters are constant. Stainless steel is chosen to be the material for flywheel, as it produces the highest torque for this preliminary calculation for material selection. Furthermore, stainless steel has the lowest value of bulk conductivity compared to the other two materials. As a generator which is attached to the magnets, it will produce electromagnetic fields during the rotation of the flywheel and the shaft. Low value of bulk conductivity will increase the strength of the electromagnetic field.

Table 4.1 Calculation of torque of the possible materials of flywheel

<b>Flywheel Material</b>	<b>Cast Iron</b>	<b>Stainless Steel</b>	<b>Aluminium</b>
<b>Bulk conductivity</b>	1500000 siemens/m	1100000 siemens/m	38000000 siemens/m
<b>Density, <math>\rho</math></b>	7300 kg/m <sup>3</sup>	8000 kg/m <sup>3</sup>	2700 kg/m <sup>3</sup>
<b><math>I_{flywheel}</math></b>	0.5333 kg.m <sup>2</sup>	0.5845 kg.m <sup>2</sup>	0.1973 kg.m <sup>2</sup>
<b><math>I_{shaft}</math></b>	1.792 x 10 <sup>-3</sup> kg.m <sup>2</sup>	1.963 x 10 <sup>-3</sup> kg.m <sup>2</sup>	6.627 x 10 <sup>-4</sup> kg.m <sup>2</sup>
<b>Torque, <math>T</math></b>	<b>0.4013 N.m</b>	<b>0.4398 N.m</b>	<b>0.1485 N.m</b>

#### 4.2.2 Mass Moment of Inertia

$$I_m = \frac{1}{2} m (r_o^2 + r_i^2)$$

Mass of flywheel,  $m = \text{volume} \times \text{density}$

The outer radius,  $r_o = 0.10$  m; the inner radius,  $r_i = 0.025$  m

The thickness of flywheel,  $t = 0.03$  m

Density of stainless steel alloy 316,  $\rho = 8000 \text{ kg/m}^3$

$$m = [(\pi r^2 h)_{outer} - (\pi r^2 h)_{inner}] \times \rho$$

$$m = [(\pi \times 0.03 \text{ m})][(0.10 \text{ m})^2 - (0.025 \text{ m})^2] \times 8000 \text{ kg/m}^3$$

$$m = 7.07 \text{ kg}$$

$$I_m = \frac{1}{2} (7.07 \text{ kg}) [(0.10 \text{ m})^2 + (0.025 \text{ m})^2]$$

$$I_m = 0.0376 \text{ kg.m}^2$$

### 4.2.3 Burst Speed

$$V = \sqrt{10 \times S}$$

$S =$  Tensile stress of flywheel's material = 89900 psi

$$= \sqrt{10 \times 89900 \text{ psi}}$$

$$= 948.16 \frac{\text{ft}}{\text{sec}} \times \frac{0.3048 \text{ m}}{1 \text{ ft}}$$

$$= 289 \text{ m/s}$$

Since  $V =$  Circumference of flywheel  $\times \omega$ , maximum angular velocity can be determined.

$$V = \pi.D \times \omega$$

$$\omega = 289 \text{ m/s} \div (\pi \times 0.20 \text{ m}) = 459.96 \text{ rad/s or } 4392 \text{ rpm}$$

### 4.2.4 Amount of Energy Required

$$E_k = \frac{1}{2} I (\omega^2)$$

$$\omega = 4392 \text{ rpm or } 459.96 \text{ rad/s}$$

$$\text{Therefore, } E_k = \frac{1}{2} (0.0376 \text{ kg.m}^2)(459.96 \text{ rad/s})^2$$

$$E_k = 3977.39 \text{ J or } 3.98 \text{ kJ}$$

Energy density =  $E/m$

$$\begin{aligned} \text{Energy density} &= 3977.39 \text{ J} \div 7.31 \text{ kg} \\ &= 544.10 \text{ J/kg} \end{aligned}$$

### 4.2.5 Flywheel Geometry

The flywheel geometry as shown in Figure 4.2 is a solid cylindrical disc, with hollow circular cross section to insert the rotating shaft. The outer diameter is 0.20 m, the inner diameter is 0.05 m, and the thickness of the flywheel is 0.03 m.

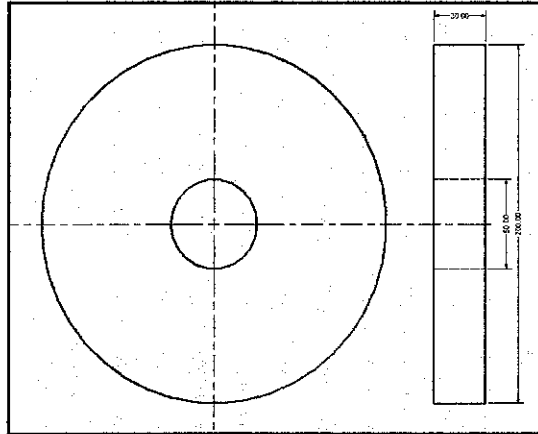


Figure 4.2: Flywheel Geometry

### 4.2.6 Stresses in Flywheel

As a rotating disc, flywheel experiences centrifugal stresses which act upon its distributed mass. It tends to pull it apart while rotating. The following are the calculations of tensile stress, maximum principal stress, maximum tangential stress, and maximum radial stress of the flywheel.

#### 1. Tensile Stress

Tensile stress is a type of stress in which the two sections of material on either side of a stress plane tend to pull apart from each other.

$$\sigma_t = \rho \times r^2 \times \omega^2$$

$$r, \text{ mean radius} = (0.10 \text{ m} + 0.025 \text{ m}) \div 2 = 0.0625 \text{ m}$$

$$\sigma_t = 8000 \text{ kg/m}^3 \times (0.0625 \text{ m})^2 \times (459.96 \text{ rad/s})^2$$

$$\sigma_t = 6611350 \text{ Pa}$$

$$\sigma_t = \mathbf{6.61 \text{ MPa}}$$

## 2. Maximum Principal Stress

The maximum principal stress is the maximum value of normal stress which acts upon a point on the flywheel disc, at right angles to the principal plane of stress.

$$\sigma_{max} = [(3 + \nu) \cdot \rho \cdot V^2] \div 8$$

$$V^2 = r^2 \omega^2 = (0.10 \text{ m})^2 \times (459.96 \text{ rad/s})^2 \\ = 2115.63 \text{ m}^2/\text{s}^2$$

$$\nu = 0.3$$

$$\sigma_{max} = [(3 + 0.3) \cdot 8000 \text{ kg/m}^3 \cdot 2115.63 \text{ m}^2/\text{s}^2] \div 8$$

$$\sigma_{max} = 6981579 \text{ Pa}$$

$$\sigma_{max} = \mathbf{6.98 \text{ MPa}}$$

Since the value of calculated tensile stress is less than the maximum principal stress, the design of flywheel with the mentioned dimension and geometry is safe to be used.

## 3. Maximum Tangential Stress

As a rotating body, flywheel generates stress along the tangent of its structure, which tends to pull it apart. It acts perpendicular to the tangent and changes the direction of the motion, without changing the velocity.

$$\sigma_{t \max} = \frac{\gamma \omega^2}{4g} [(3 + \mu) r_o^2 + (1 - \mu) r_i^2]$$

$$g = 9.81 \text{ m/s}^2$$

$$\gamma = 8000 \text{ kg/m}^3 \times 9.81 \text{ N/kg} = 78480 \text{ N/m}^3$$

$$\mu = 0.3 \text{ (Poisson's ratio)}$$

$$\sigma_{t \max} = \frac{(78480 \text{ N/m}^3)(459.96 \text{ rad/s})^2}{4 \times 9.81 \text{ m/s}^2} [(3 + 0.3)(0.10 \text{ m})^2 + (1 - 0.3)(0.025 \text{ m})^2]$$

$$\sigma_{t \max} = 423126403.2 \text{ N/m}^4 (0.03344 \text{ m}^2)$$

$$\sigma_{t \max} = 14149346.92 \text{ Pa}$$

$$\sigma_{t \max} = \mathbf{14.1 \text{ MPa}}$$

#### 4. Maximum Radial Stress

Radial stress which occurs on rotating discs acts towards or away from the flywheel's central axis.

$$\sigma_{r \max} = \frac{3+\nu}{8} \times \rho \omega^2 (r_o^2 - r_i^2)$$

$$\nu = 0.3 \text{ (Poisson's ratio)}$$

$$\sigma_{r \max} = \frac{3+0.3}{8} \times [(8000 \text{ kg/m}^3) \times (459.96 \text{ rad/s}^2)^2] \times [(0.20 \text{ m})^2 - (0.025 \text{ m})^2]$$

$$\sigma_{r \max} = 0.4125 \times 66642408.5$$

$$\sigma_{r \max} = 27489993.51 \text{ Pa}$$

$$\sigma_{r \max} = \mathbf{27.5 \text{ MPa}}$$

Table 4.2 summarizes the stresses in flywheel as calculated previously.

Table 4.2: Summary of stresses in flywheel

Stresses in Flywheel	Values
Tensile Stress, $\sigma_t$	6.61 MPa
Maximum Principal Stress, $\sigma_{max}$	6.98 MPa
Maximum Tangential Stress, $\sigma_{t \max}$	14.1 MPa
Maximum Radial Stress, $\sigma_{r \max}$	27.5 MPa



### 4.3 Shaft Design Calculation

#### 4.3.1 Torsion Moment

For a shaft that delivers 50 hp power for rotation, the torsion moment can be calculated:

$$M_t = \frac{W}{\omega}$$

$$50 \text{ hp} \times 745.7 \text{ W} = 37285 \text{ W}$$

$$M_t = \frac{37285 \text{ W}}{459.96 \text{ rad/s}} = 81.06 \text{ N.m}$$

#### 4.3.2 Free Body Diagram

Figure 4.3 shows the free body diagram of FESS's structure with the following shaft dimensions:

$$a = 0.15 \text{ m}; b = 0.15 \text{ m}; c = 0.10 \text{ m}$$

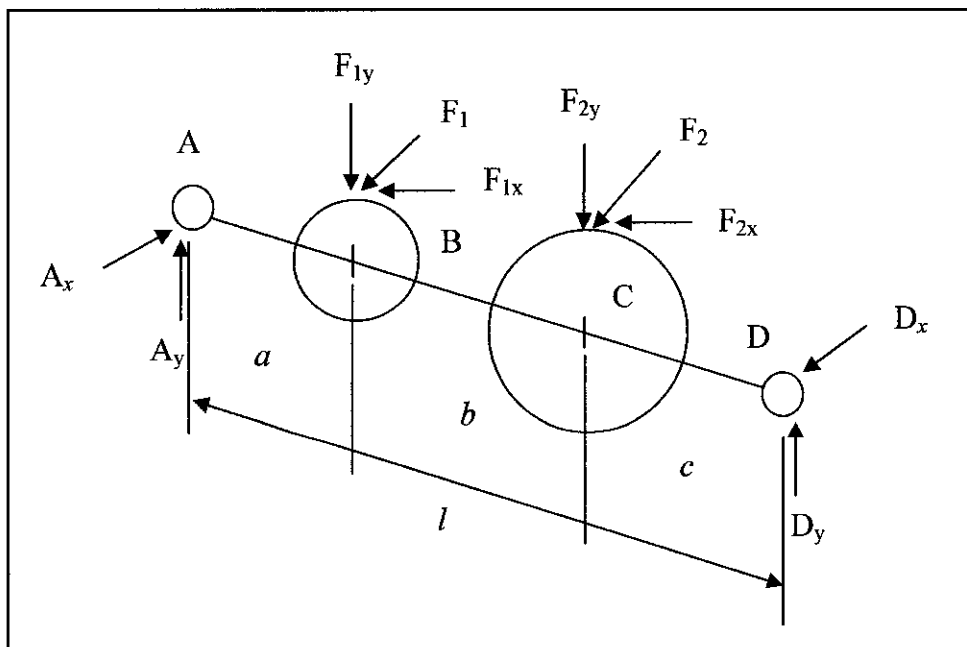


Figure 4.3: Free Body Diagram of FESS

### 4.3.3 Shaft Loading

Torsion moment,  $M_t = 81.06 \text{ N.m}$

Pressure angle,  $\alpha = 20^\circ$

Radius of shaft,  $r_1 = 0.0175 \text{ m}$

Radius of shaft,  $r_2 = 0.025 \text{ m}$

#### 1. Circumferential and radial forces

$$\begin{aligned} F_{1x} &= M_t \div r_1 \\ &= 81.06 \text{ N.m} \div 0.0175 \text{ m} = 4632 \text{ N} \end{aligned}$$

$$F_{1y} = F_{1x} \times \tan \alpha = 1686 \text{ N}$$

$$\begin{aligned} F_1 &= \sqrt{(4632 \text{ N})^2 + (1686 \text{ N})^2} \\ &= 4929 \text{ N} \end{aligned}$$

$$\begin{aligned} F_{2x} &= M_t \div r_2 \\ &= 81.06 \text{ N.m} \div 0.025 \text{ m} = 3242 \text{ N} \end{aligned}$$

$$F_{2y} = F_{2x} \times \tan \alpha = 1180 \text{ N}$$

$$\begin{aligned} F_2 &= \sqrt{(3242 \text{ N})^2 + (1180 \text{ N})^2} \\ &= 3450 \text{ N} \end{aligned}$$

#### 2. Reactions at point A (Bearing)

$$\begin{aligned} A_x &= [F_{1x} \times (b + c) + F_{2x} \times c] \div l \\ &= [(4053 \text{ N} \times 0.30 \text{ m}) + (3242 \text{ N} \times 0.10 \text{ m})] \div 0.40 \text{ m} \\ &= 3850 \text{ N} \end{aligned}$$

$$\begin{aligned} A_y &= [F_{1y} \times (b + c) + F_{2y} \times c] \div l \\ &= [(1475 \text{ N} \times 0.30 \text{ m}) + (1180 \text{ N} \times 0.10 \text{ m})] \div 0.40 \text{ m} \\ &= 1401 \text{ N} \end{aligned}$$

### 3. Reactions at point D (Bearing)

$$\begin{aligned}D_x &= [F_{1x} \times a + F_{2x} \times (a + b)] \div l \\&= [(4053 \text{ N} \times 0.15 \text{ m}) + (3242 \text{ N} \times 0.30 \text{ m})] \div 0.40 \text{ m} \\&= 3945 \text{ N}\end{aligned}$$

$$\begin{aligned}D_y &= [F_{1y} \times a + F_{2y} \times (a + b)] \div l \\&= [(1475 \text{ N} \times 0.15 \text{ m}) + (1180 \text{ N} \times 0.30 \text{ m})] \div 0.40 \text{ m} \\&= 1438 \text{ N}\end{aligned}$$

### 4. Bending moments at section B (Driver)

$$M_{Bx} = A_x \times a = 3850 \text{ N} \times 0.15 \text{ m} = 577.50 \text{ N.m}$$

$$M_{By} = A_y \times a = 1401 \text{ N} \times 0.15 \text{ m} = 210.15 \text{ N.m}$$

$$\begin{aligned}M_B &= \sqrt{M_{Bx}^2 + M_{By}^2} = \sqrt{(577.50 \text{ N.m})^2 + (210.15 \text{ N.m})^2} \\&= 614.55 \text{ N.m}\end{aligned}$$

### 5. Bending moments at section C (Flywheel Disc)

$$M_{Cx} = D_x \times c = 3945 \text{ N} \times 0.10 \text{ m} = 394.5 \text{ N.m}$$

$$M_{Cy} = D_y \times c = 1438 \text{ N} \times 0.10 \text{ m} = 143.8 \text{ N.m}$$

$$\begin{aligned}M_C &= \sqrt{M_{Cx}^2 + M_{Cy}^2} = \sqrt{(394.5 \text{ N.m})^2 + (143.8 \text{ N.m})^2} \\&= 419.89 \text{ N.m}\end{aligned}$$

### 6. Bending Stress

i) On the driver

$$\sigma_b = \frac{M_b c}{I}$$

$$I = \frac{\pi \times d^4}{64} = \frac{\pi(0.035 \text{ m})^4}{64} = 7.366 \times 10^{-8} \text{ m}^4$$

$$\sigma_b = \frac{(614.55 \text{ N.m})(0.0175 \text{ m})}{7.366 \times 10^{-8} \text{ m}^4}$$

$$\sigma_b = 146 \text{ MPa}$$

ii) On the flywheel disc

$$\sigma_b = \frac{M_c c}{I}$$

$$I = \frac{\pi \times d^4}{64} = \frac{\pi(0.05 \text{ m})^4}{64} = 3.068 \times 10^{-7} \text{ m}^4$$

$$\sigma_b = \frac{(614.55 \text{ N.m})(0.025 \text{ m})}{3.068 \times 10^{-7} \text{ m}^4}$$

$$\sigma_b = 50.01 \text{ MPa}$$

## 7. Torsional Shear Stress

i) On the driver

$$S_s = \frac{Tc}{J}$$

$$J = \text{Polar moment of inertia} = \frac{\pi \times d^4}{32}$$

$$= \frac{\pi \times (0.035 \text{ m})^4}{32} = 1.47 \times 10^{-7} \text{ m}^4$$

c = radius of the shaft

$$S_s = \frac{81.06 \text{ N.m} \times 0.0175 \text{ m}}{1.47 \times 10^{-7} \text{ m}^4} = 9650000 \text{ Pa} = 9.65 \text{ MPa}$$

ii) On the flywheel disc

$$S_s = \frac{Tc}{J}$$

$$J = \text{Polar moment of inertia} = \frac{\pi \times d^4}{32}$$

$$= \frac{\pi \times (0.05 \text{ m})^4}{32} = 6.14 \times 10^{-7} \text{ m}^4$$

c = radius of the shaft

$$S_s = \frac{81.06 \text{ N.m} \times 0.025 \text{ m}}{6.14 \times 10^{-7} \text{ m}^4} = 3300489 \text{ Pa} = 3.30 \text{ MPa}$$

## 8. Shear Stress

i) On the driver

$$\tau = \frac{16T}{\pi D^3}$$

$$\tau = \frac{16(81.06 \text{ N.m})}{\pi(0.035 \text{ m})^3}$$

$$\tau = 9628809.10 \text{ Pa} = 9.63 \text{ MPa}$$

ii) On the flywheel disc

$$\tau = \frac{16T}{\pi D^3}$$

$$\tau = \frac{16(81.06 \text{ N.m})}{\pi(0.05 \text{ m})^3}$$

$$\tau = 3302681.52 \text{ Pa} = 3.30 \text{ MPa}$$

## 9. Angle of Twist

$$\theta = \frac{TL}{GJ}$$

Torque applied,  $T = 81.06 \text{ N.m}$

Length of shaft,  $L = 0.4 \text{ m}$

Shear modulus of elasticity,  $G = 193 \text{ GPa}$

i) On the driver

Polar moment of inertia,  $J = 1.47 \times 10^{-7} \text{ m}^4$

$$\theta = \frac{(81.06 \text{ N.m})(0.4 \text{ m})}{(193 \times 10^9 \text{ Pa})(1.47 \times 10^{-7} \text{ m}^4)}$$

$$\theta = 0.001143 \text{ rad} = 0.0655^\circ$$

ii) On the flywheel disc

Polar moment of inertia,  $J = 6.14 \times 10^{-7} \text{ m}^4$

$$\theta = \frac{(81.06 \text{ N.m})(0.4 \text{ m})}{(193 \times 10^9 \text{ Pa})(6.14 \times 10^{-7} \text{ m}^4)}$$

$$\theta = 0.0002736 \text{ rad} = 0.0157^\circ$$

All the values of forces, bending moments, torque, and reaction supports calculated previously are applied on specific locations along the shaft, as shown in Figure 4.4 and Figure 4.5 below. The graphs generated are shown in Figure 4.6, 4.7, 4.8, 4.9, and 4.10.

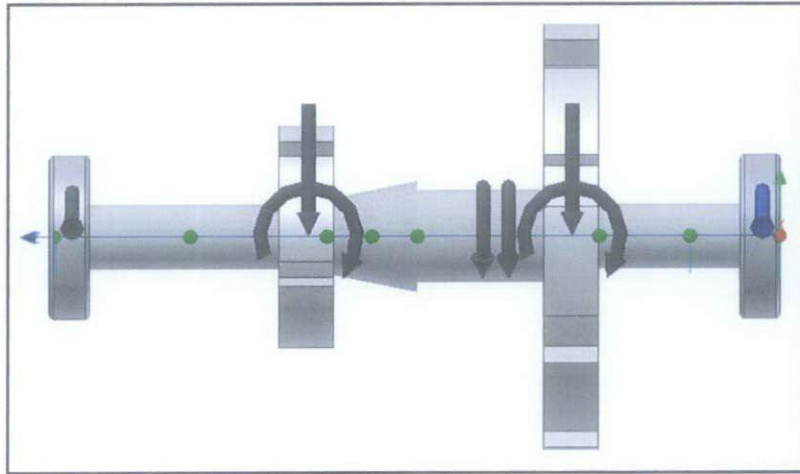


Figure 4.4: Applied loads and supports on shaft

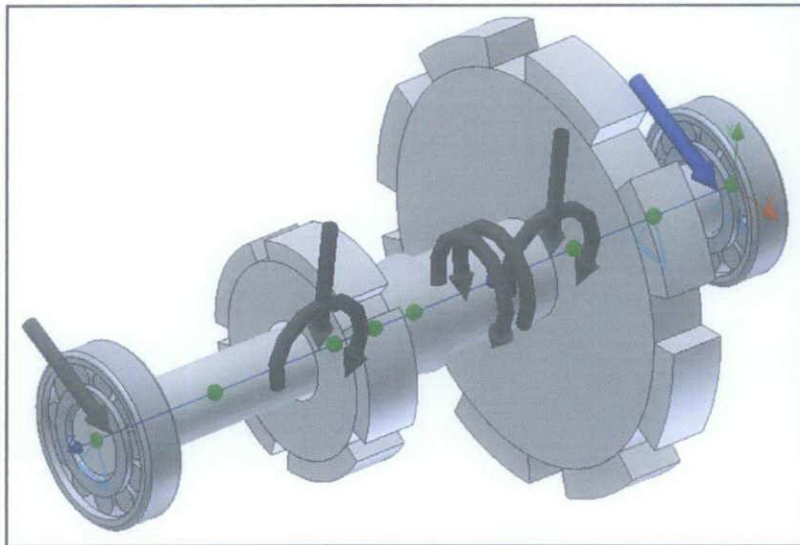


Figure 4.5: Applied loads and supports on shaft in 3D view

In Figure 4.6, the maximum shear force is 8897.02 N which occurs near the fixed support at the bearing. The minimum shear force is 3450 N which occurs at the flywheel disc.

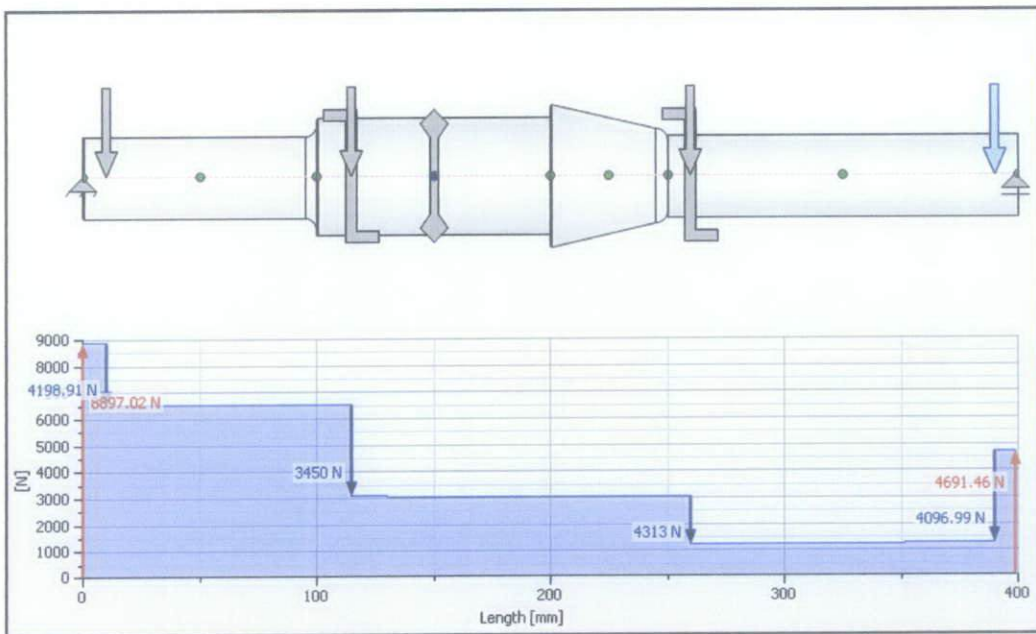


Figure 4.6: Shear Force Diagram

The maximum bending moment as in Figure 4.7 is 802.726 N.m which occurs at the driver due to the force which is imposed on it. Since the bending moment of the driver is calculated to be 614.55 N.m, it will not experience bending while operating.

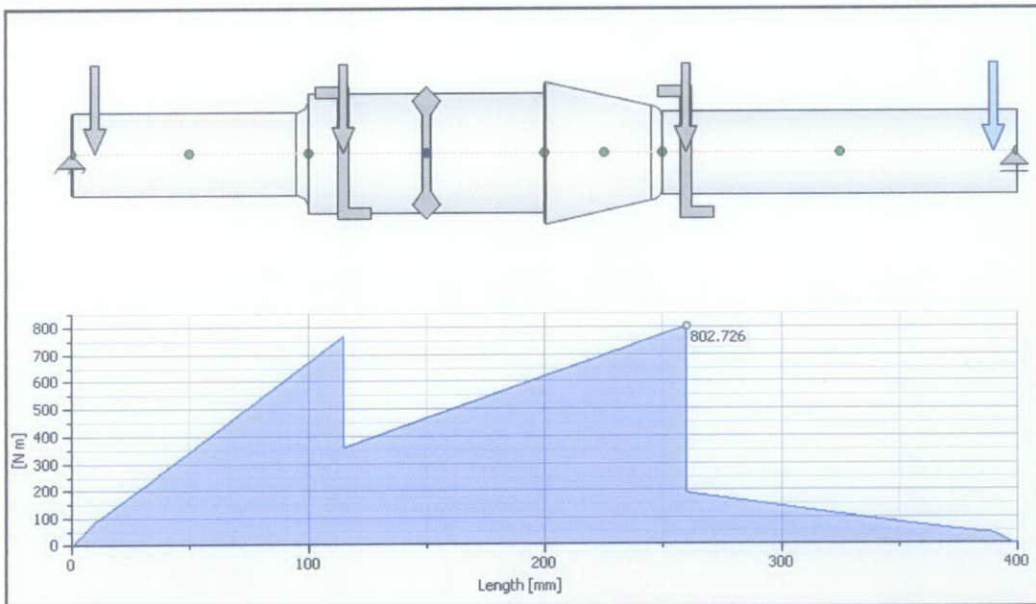


Figure 4.7: Bending Moment Diagram

In Figure 4.8, the maximum bending stress is 190.705 MPa, which occurs on the driver. The bending stress is due to the rotation of the shaft which transmits power and the force which is applied on the driver itself. Based on the previous calculation, the bending stress at the driver is 146 MPa, whereas the bending stress at the flywheel is 50.01 MPa. Since both calculations do not exceed the maximum bending stress, the design is safe to be used.

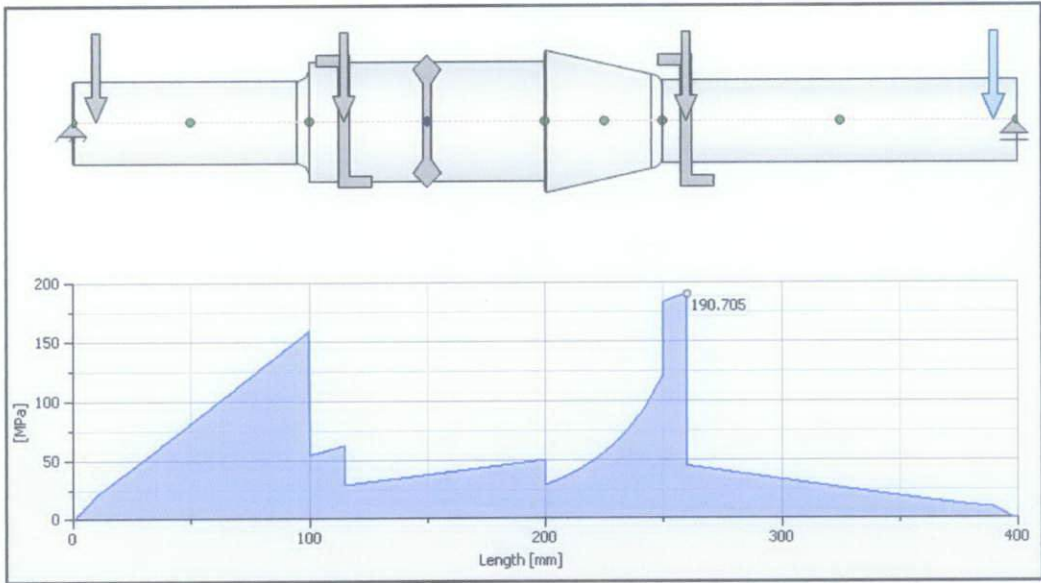


Figure 4.8: Bending Stress Diagram

Referring to Figure 4.9, the highest deflection angle occurs near the fixed support, which is the cylindrical roller bearing, with a very small value of  $0.193627^{\circ}$ . Along the shaft, the deflection angle decreases until it reaches the minimum value of  $0.00163809^{\circ}$ , at the centre of the shaft. Then, the value increases again, but in such a small value. This clearly shows that the shaft design is safe, as it will not break when it rotates, especially at its centre.



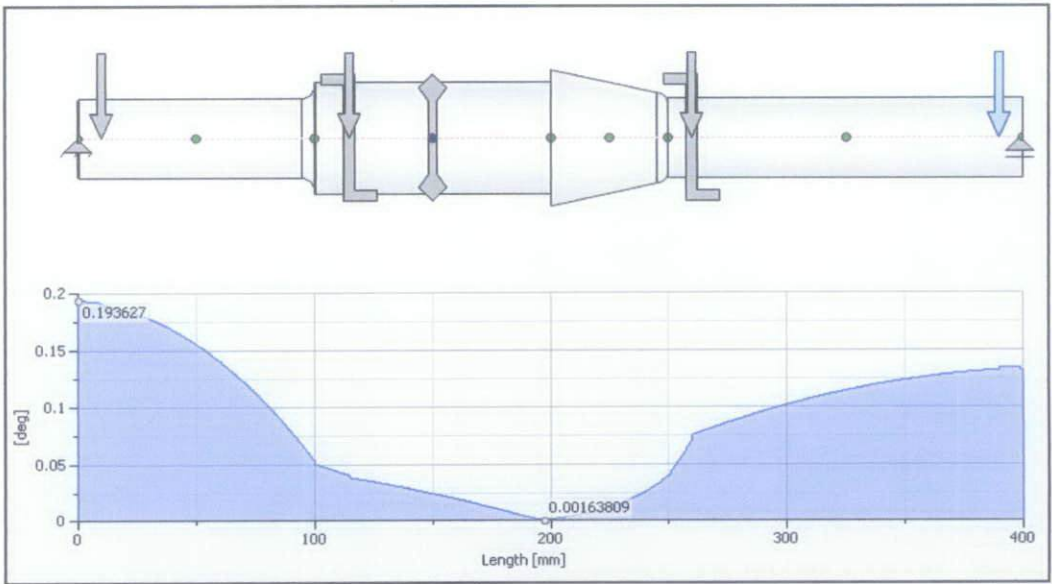


Figure 4.9: Deflection Angle Diagram

The maximum deflection, 295.541 micron occurs at the cross section of shaft, where the diameter changes, at length of 200 mm. Since the value is very small, it can be neglected. This shows that the shaft structure only experiences a small value of deflection during its operation.

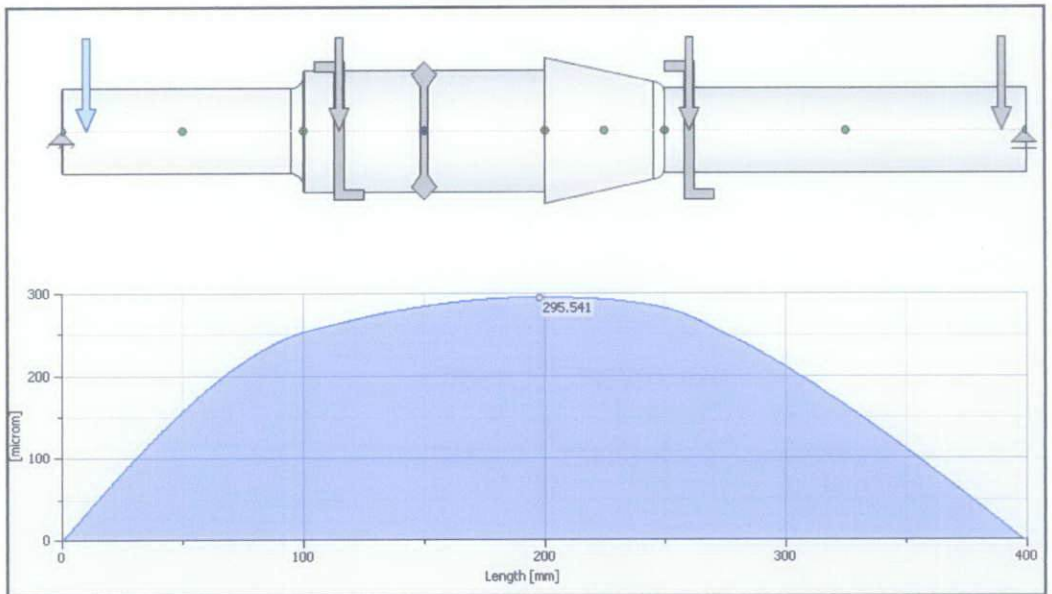


Figure 4.10: Deflection Diagram

#### 4.4 Detailed Design

Figure 4.11 shows the detailed design of flywheel energy storage system structure, while Table 4.3 shows the design's parts' list

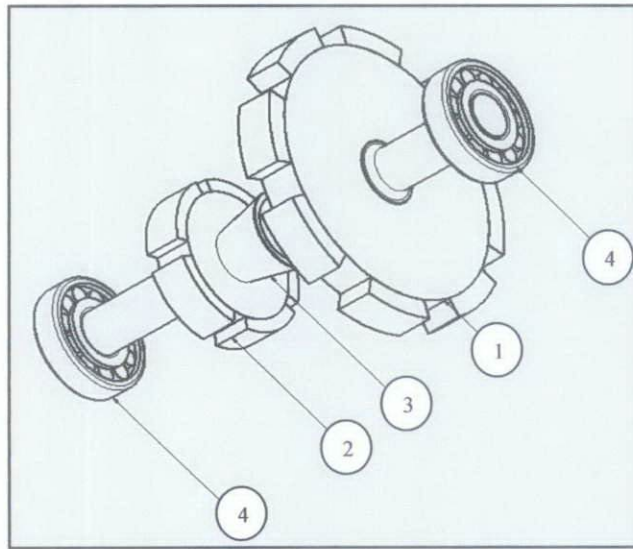


Figure 4.11: Detailed Design of Flywheel Energy Storage System Structure

Table 4.3: Design's parts' list

PARTS' LIST		
Item	Quantity	Part's Name
1	1	Flywheel Disc with magnets attached
2	1	Driver with magnets attached
3	1	Shaft
4	2	SKF Series CRM – SKF CRM 11A (Cylindrical Roller Bearing)

## 4.5 Static and Dynamic Analyses

Figure 4.12 shows the geometry and meshing of FESS structure. The number of nodes is 73692 and the number of elements is 22137. Meshing are important in the analysis using ANSYS 11.0 Software because it allows the parts to be in finite elements and the distribution of mechanical properties such as the stress, strain, temperature, energy, and so on can be observed and analysed accurately.

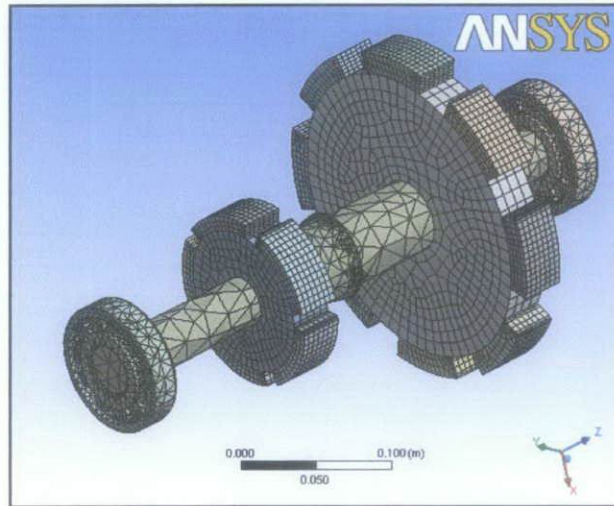


Figure 4.12: Geometry and Meshing of FESS

The maximum total deformation as in Figure 4.13 occurs at the outer parts of flywheel disc, with the value of  $4.3907 \times 10^{-4}$  m. Minimum total deformation, 0 m occurs at both ends of the cylindrical roller bearings, since they are fixed constraints.

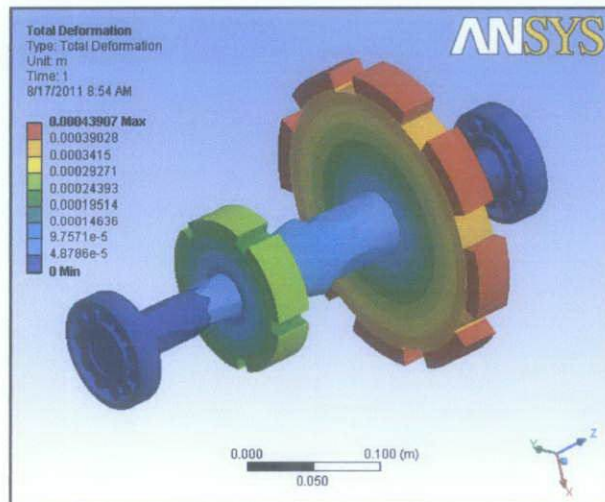


Figure 4.13: Total Deformation

The maximum principal stress is 6.95 MPa which occurs at both bearings, the outer part of driver and also the outer part of flywheel as shown in Figure 4.14. The calculated maximum principal stress is slightly the same with the simulation, therefore, the results is validated to be true.

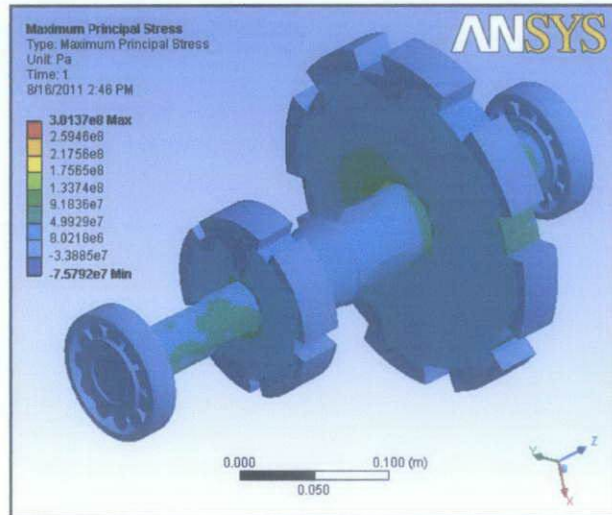


Figure 4.14: Maximum Principal Stress

In Figure 4.15, the maximum shear stress occurs at the driver with a value of 187.68 MPa, whereas the minimum shear stress, 0.769 MPa occurs at both bearings. Based on the calculation, the driver produces shear stress of 9.63 MPa, whereas flywheel disc produce 3.30 MPa. Both calculations do not exceed the maximum shear stress, thus the design is safe to function.

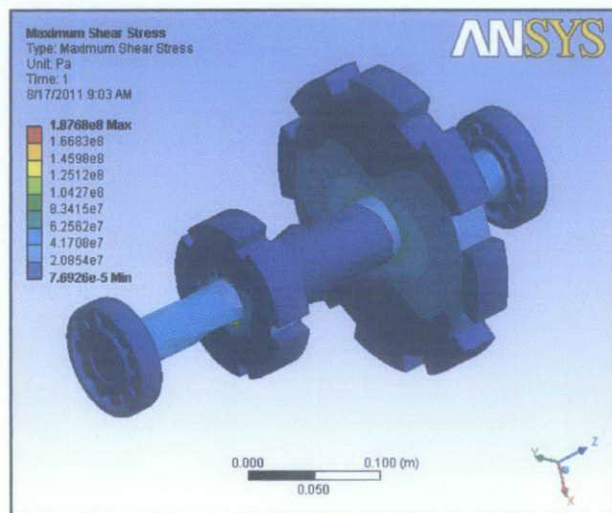


Figure 4.15: Maximum Shear Stress



The strain energy is the potential energy stored in the material before it deforms. Based on Figure 4.16, the maximum strain energy,  $4.0099 \times 10^{-2}$  J occurs at the shaft, near the connection with the flywheel disc. The minimum strain energy,  $3.4996 \times 10^{-11}$  J occurs at both ends of the cylindrical roller bearings. As one of the essential element of the system, the shaft is safe to be used since it possesses the highest strain energy. This shows that the shaft can withstand the load imposed on it.

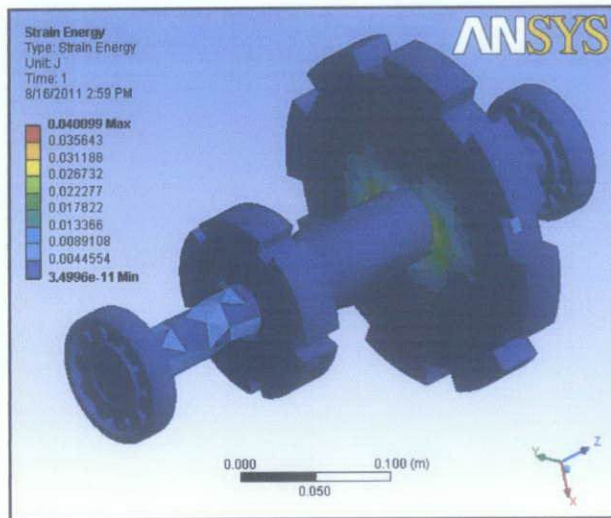


Figure 4.16: Strain Energy

Referring to Figure 4.17, the maximum total acceleration,  $8.7088 \times 10^{-4}$  m/s<sup>2</sup> occurs at the outer radial part of the flywheel. This is due to the tangential force which induced rotation to the flywheel disc.

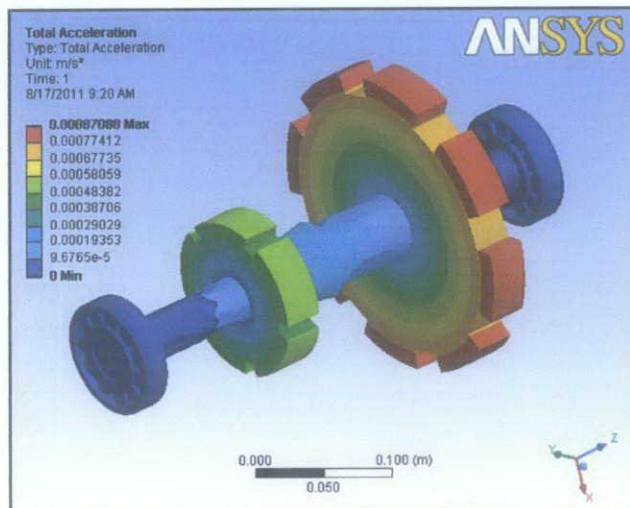


Figure 4.17: Total Acceleration

## 4.6 Final Design Specifications

Figure 4.18 shows the final design in 3D view, whereas Figure 4.19 shows the base view and projected views of the final design.

### 4.6.1 Final Design Geometry

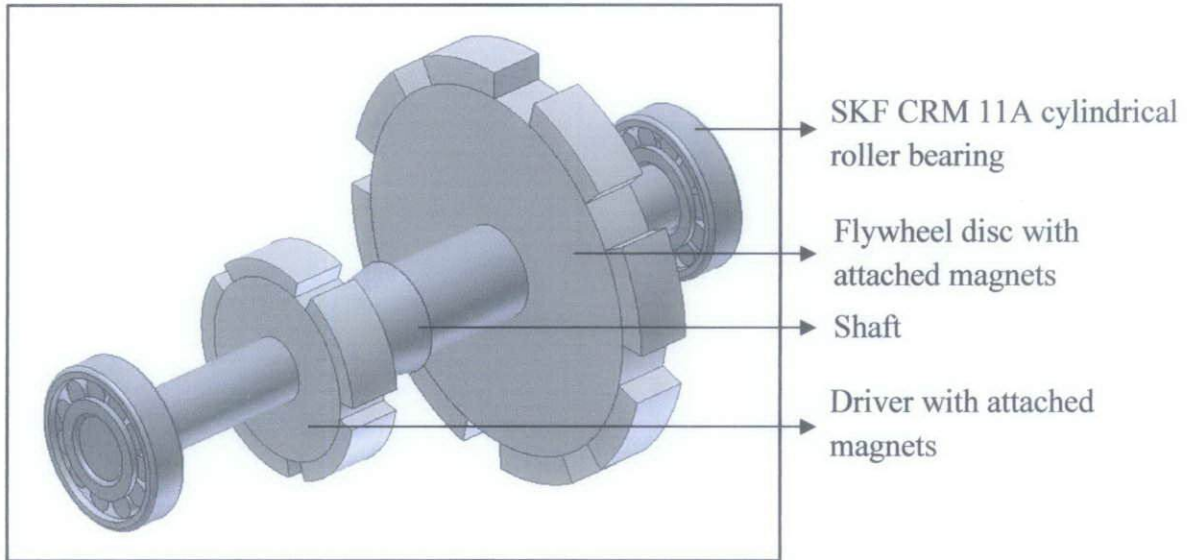


Figure 4.18: Final design in 3D view

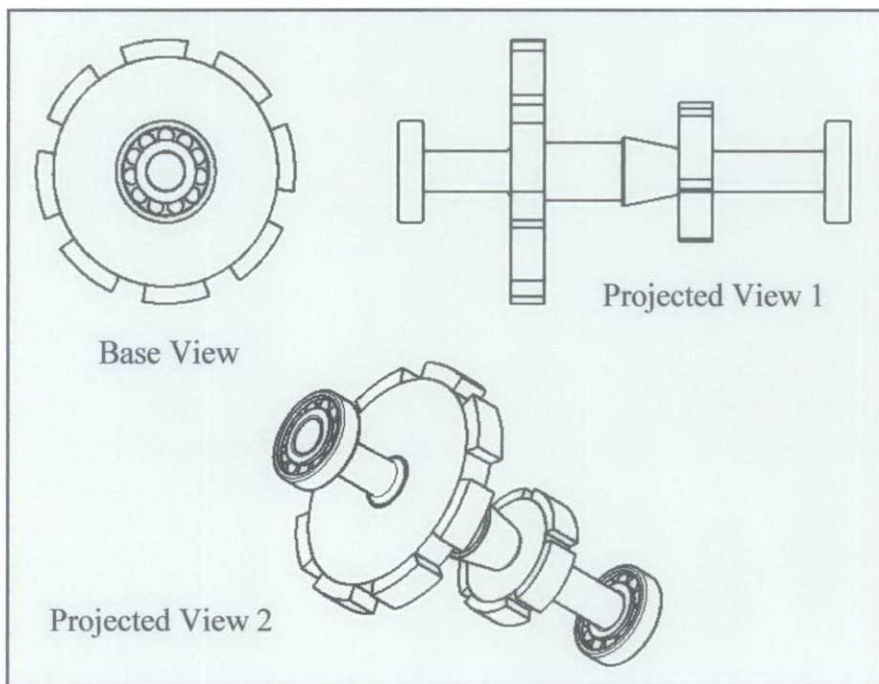


Figure 4.19: Base view and projected views of final design

#### 4.6.2 Flywheel Disc

Table 4.4 is the summary of the flywheel disc specifications based on previous calculations.

Table 4.4: Flywheel Disc Specifications

<b>Mass, <math>m</math></b>	7.07 kg
<b>Thickness, <math>t</math></b>	0.03 m
<b>Outer Diameter, <math>D_o</math></b>	0.20 m
<b>Outer Radius, <math>r_o</math></b>	0.10 m
<b>Inner Diameter, <math>D_i</math></b>	0.05 m
<b>Inner Radius, <math>r_i</math></b>	0.025 m
<b>Density of Stainless Steel, <math>\rho</math></b>	8000 kg/m <sup>3</sup>
<b>Bulk Conductivity</b>	1100000 siemens/m
<b>Mass Moment of Inertia, <math>I_m</math></b>	0.0376 kg.m <sup>2</sup>
<b>Burst Speed, <math>S</math></b>	289 m/s
<b>Angular Velocity (Maximum), <math>\omega</math></b>	459.96 rad/s or 4392 rpm
<b>Energy Required, <math>E_k</math></b>	3977.97 J or 3.98 kJ
<b>Energy Density</b>	562.57 J/kg
<b>Tensile Stress, <math>\sigma_t</math></b>	6.61 MPa
<b>Maximum Principal Stress, <math>\sigma_{max}</math></b>	6.98 MPa
<b>Maximum Tangential Stress, <math>\sigma_{t max}</math></b>	14.1 MPa
<b>Maximum Radial Stress, <math>\sigma_{r max}</math></b>	27.5 MPa

### 4.6.3 Shaft

Table 4.5 shows the summary of the shaft forces and reaction supports, while Table 4.6 is the shaft loadings on driver and flywheel disc. Tables 4.4, 4.5, and 4.6 are based on the previous calculations and analyses by the softwares.

Table 4.5: Shaft Forces and Reaction Supports

<b>Power, <math>P</math></b>	50 hp or 37285 W
<b>Torsional Moment, <math>M_t</math></b>	81.06 N.m
<b>Length, <math>L</math></b>	0.4 m
<b><math>F_1</math></b>	4929 N
<b><math>F_2</math></b>	3450 N
<b><math>A_x</math></b>	3850N
<b><math>A_y</math></b>	1401 N
<b><math>D_x</math></b>	3945 N
<b><math>D_y</math></b>	1438 N

Table 4.6: Shaft Loadings on Driver and Flywheel Disc

<b>Properties</b>	<b>Driver</b>	<b>Flywheel Disc</b>
<b>Bending Moment, <math>M</math></b>	614.55 N.m	419.89 N.m
<b>Bending Stress, <math>\sigma_b</math></b>	146 MPa	50.01 MPa
<b>Torsional Shear Stress, <math>S_s</math></b>	9.65 MPa	3.30 MPa
<b>Shear Stress, <math>\tau</math></b>	9.63 MPa	3.30 MPa
<b>Angle of Twist, <math>\theta</math></b>	0.0655 <sup>0</sup>	0.0157 <sup>0</sup>

The most suitable material to design a flywheel disc is stainless steel, which has high density and low bulk conductivity. High density material gives a high value of mass moment of inertia, thus provides large torque. On the other hand, since the value of stainless steel's bulk conductivity is low, it can increase the strength of the electromagnetic field, since rotations are induced by the electromagnetic flux generated by the interaction between the magnets and coils that surround it.



The burst speed or the critical speed of the flywheel is 289 m/s, whereas the maximum angular velocity is 459.96 rad/s or 4392 rpm. Since the value of the angular velocity is quite high, the kinetic energy that is stored also has a high value, which is 3.98 kJ. The energy density is also high, which is 562.57 J/kg. The higher the value of energy density, more energy can be stored in the flywheel itself.

The calculated maximum principal stress is 6.98 MPa, whereas the maximum principal stress value generated from simulation by ANSYS 11.0 Software is 6.95 MPa. There is not much different between the values, therefore, the calculation and the simulation is validated to be true. Since the tensile stress is 6.61 MPa and it does not exceed the maximum principal stress, the design is safe to be operated.

With respect to the shaft design, based on the power required, which is 50 hp or 37285 W, the torsion moment produced is 81.06 N.m. The forces which act on the driver and the flywheel disc, and the reaction forces on both bearings can be calculated. From these values, bending moment, bending stress, torsional shear stress, shear stress, and angle of twist can be determined. The calculated results are compared with the analysis and diagrams generated by Autodesk Inventor Professional Software.

It is observed that the values which are calculated do not exceed the maximum value based on the analyses by the software. This shows that, the design is safe and can function in the future. Furthermore, the value of deflection and the deflection angle on the shaft is very small and can be neglected. This reflects that the shaft can withstand the loads imposed on it and will not break during rotation.

Further static and dynamic analyses are conducted to verify this using the ANSYS 11.0 Software, where during the simulation, the total deformation is as small as  $4.3907 \times 10^{-4}$  m and the shaft does not break while rotating. The maximum shear stress as generated by the software also has a higher value than that of the calculated one, thus shows that the design is safe to function. The strain energy or the potential energy stored in the material before it deforms also shows the highest value at the shaft, near the joint with flywheel disc. Therefore, the shaft is strong enough to withstand the loads imposed on it.

## **CHAPTER 5**

### **CONCLUSIONS AND RECOMMENDATIONS**

As a conclusion for this final year project, this dissertation includes the design and analysis of flywheel energy storage system's structure as possible alternative energy in the future which can reduce the green house gas emissions besides giving a perpetual motion to the system. The design approaches include calculations of loads imposed on the shaft and flywheel based on free body diagram and comparison with the result and analyses which are generated by Autodesk Inventor Professional Software and ANSYS 11.0 Software. The final design specifications show that stainless steel is the most suitable material for flywheel disc as it produces the highest torque and can increase the strength of electromagnetic field induced due to its low bulk conductivity. The kinetic energy that is stored has a high value, which is 3.98 kJ, thus produces high energy density of 562.57 J/kg which can store more energy, as well as sustaining the motion of the flywheel energy storage system. Since the comparisons of results between the calculations and the software mentioned do not exceed the maximum values, the design is verified and is safe to be operated in the future. Regarding the future work for continuation, it is highly recommended to include further analysis of the electromagnetic flux induced by the system so that the amount of voltage produced can be determined, besides calculations of wiring in the driver or the motor system, the winding of the wire, and to come out with several configurations of flywheel energy storage system which can give the highest efficiency.

## REFERENCES

- Ashley S. (1993). Flywheel put a new spin on electric vehicles. *Mech Eng* : 44-51.
- Anerdi G, Brusaglino G. (1994). Technology potential of flywheel storage and application impact on electric vehicles. In: *12<sup>th</sup> international electric vehicle symposium (EVS-12), vol. 1*, p. 37-47.
- Charles E.B (Engineering Science and Mechanics). Composite Flywheel Energy Storage. Retrieved on August 1, 2010, from <http://www.esm.psu.edu/labs/cmtc/flywheel.html>
- Christopher DA, Beach R. (1998). Flywheel technology development program for aerospace applications. *IEEE AES System Magazine*; 13(6):9-14.
- DeTersa SJ. (1999, November). Materials for advanced flywheel energy-storage devices. *MRS Bull* : 51-5.
- Diesel rotary uninterruptible power supply. (2011, March 29) Retrieved on May 25, 2011 from [http://en.wikipedia.org/wiki/Diesel\\_rotary\\_uninterruptible\\_power\\_supply](http://en.wikipedia.org/wiki/Diesel_rotary_uninterruptible_power_supply)
- George Y, Baaklini, et al. (2000, October). NDE Methodologies for composite flywheels certification. *NASA/TM 2000-210473*.
- Juvinall, R. C., Marshek, K. M. (1991). Fundamentals of machine component design. The U.S.A.: Hamilton Printing Company.
- Kojima A, et al. (1997). Flywheel energy storage system. In *5<sup>th</sup> Japan international SAMPE symposium*, p. 249-52, Tokyo.

M. F. Spotts, T. E. Shoup (1998). *Design of machine elements* (7<sup>th</sup> ed.). New Jersey: Prentice-Hall.

Moritz B. (1998, March/April). Composites maximize energy storage in industrial flywheels. *Composites* : 21-4.

Punch B. and Goodman E. Composite Flywheel Design, Retrieved on August 1, 2010 from <http://garage.cse.msu.edu/demos/index.html>

Regenerative Brake. (2011) Retrieved on May 30, 2011 from [http://en.wikipedia.org/wiki/Regenerative\\_braking](http://en.wikipedia.org/wiki/Regenerative_braking)

Rodriguez GE, Studer et al. (1983). Assessment of flywheel energy storage for space craft power system. *NASA technical memorandum*, 85062.

Sung Kyu et al. (2001). Optimum design of multi-ring composite flywheel rotor using a modified generalized plane strain assumption. *Int J Mech Sci* ;43 : 993-1007.

Uninterruptible power supply. (2011) Rotary DRUPS (diesel rotary UPS). Retrieved on May 25, 2011 from <http://www.answers.com/topic/uninterruptible-power-supply#ixzz1NM7Jlml8>.

WTEC Hyper-Librarian. (1997, September) FLYWHEELS, Diurnal Load Leveling. Retrieved on August 1, 2010 from [http://www.wtec.org/loyola/scpa/04\\_02.htm](http://www.wtec.org/loyola/scpa/04_02.htm)

## APPENDICES

### Appendix I

#### Energy stored in flywheel:

$m$  = mass of the flywheel in kg,

$k$  = radius of gyration of the flywheel in metres,

$I$  = mass moment of inertia of the flywheel about the axis of rotation in  $\text{kg.m}^2$   
 $= m.k^2$ ,

$N_1$  and  $N_2$  = Maximum and minimum speeds during the cycle in r.p.m.,

$\omega_1$  and  $\omega_2$  = Maximum and minimum angular speeds during cycle, in rad/s,

$N$  = Mean speed during the cycle in r.p.m. =  $\frac{N_1 + N_2}{2}$

$\omega$  = Mean angular speed during the cycle in rad/s =  $\frac{\omega_1 + \omega_2}{2}$

$C_S$  = Coefficient of fluctuation of speed =  $\frac{N_1 - N_2}{N}$  or  $\frac{\omega_1 - \omega_2}{\omega}$

Since the kinetic energy of the flywheel is:

$$E = \frac{1}{2} \times I \cdot \omega^2 = \frac{1}{2} \times m.k^2 \cdot \omega^2 \text{ (in N.m or Joules)}$$

As the speed of the flywheel changes from  $\omega_1$  and  $\omega_2$ , the maximum fluctuation of energy,

$$\Delta E = \text{Maximum K.E.} - \text{Minimum K.E.} = \frac{1}{2} I(\omega_1)^2 - \frac{1}{2} I(\omega_2)^2$$

$$= \frac{1}{2} \times I [(\omega_1)^2 - (\omega_2)^2] = \frac{1}{2} \times I (\omega_1 + \omega_2) (\omega_1 - \omega_2)$$

$$= I.\omega(\omega_1 - \omega_2) \dots\dots\dots(i)$$

$$= I.\omega^2 \left[ \frac{\omega_1 - \omega_2}{\omega} \right]$$

$$= I.\omega^2.C_S = m.k^2.\omega^2.C_S \dots\dots(ii)$$

$$= 2 E.C_S \dots\dots(ii)$$

The radius of gyration,  $k$  may be taken equal to the mean radius of the rim ( $R$ ), because the thickness of rim is very small as compared to the diameter of the rim. Therefore, by substituting  $k = R$ , in equation (ii), we would have

$$\Delta E = m.R^2.\omega^2.C_S = m.v^2.C_S$$

## Appendix 2

The preliminary calculation for material selection is based on equation (4), (5), and (6) where  $t = 0.03$  m,  $r_o = 0.20$  m,  $r_i = 0.025$  m, assume that  $\alpha = 0.75$  rad/s<sup>2</sup>.

For **cast iron** flywheel,

$$\begin{aligned} I_{\text{flywheel}} &= \frac{1}{2} (7300 \text{ kg/m}^3) \pi (0.03 \text{ m}) [(0.20 \text{ m})^2 - (0.025 \text{ m})^2]^2 \\ &= 0.5333 \text{ kg.m}^2 \end{aligned}$$

$$I_{\text{shaft}} = \frac{1}{2} (7300 \text{ kg/m}^3) \pi (0.4 \text{ m}) (0.025 \text{ m})^4 = 1.792 \times 10^{-3} \text{ kg.m}^2$$

$$T = I_{\text{total}} \alpha = (0.5333 + 0.001792) 0.75 = 0.4013 \text{ N.m}$$

For **stainless steel** flywheel,

$$\begin{aligned} I_{\text{flywheel}} &= \frac{1}{2} (8000 \text{ kg/m}^3) \pi (0.03 \text{ m}) [(0.20 \text{ m})^2 - (0.025 \text{ m})^2]^2 \\ &= 0.5845 \text{ kg.m}^2 \end{aligned}$$

$$I_{\text{shaft}} = \frac{1}{2} (8000 \text{ kg/m}^3) \pi (0.4 \text{ m}) (0.025 \text{ m})^4 = 1.963 \times 10^{-3} \text{ kg.m}^2$$

$$T = I_{\text{total}} \alpha = (0.5845 + 0.001963) 0.75 = 0.4398 \text{ N.m}$$

For **aluminium** flywheel,

$$\begin{aligned} I_{\text{flywheel}} &= \frac{1}{2} (2700 \text{ kg/m}^3) \pi (0.03 \text{ m}) [(0.20 \text{ m})^2 - (0.025 \text{ m})^2]^2 \\ &= 0.1973 \text{ kg.m}^2 \end{aligned}$$

$$I_{\text{shaft}} = \frac{1}{2} (2700 \text{ kg/m}^3) \pi (0.4 \text{ m}) (0.025 \text{ m})^4 = 6.627 \times 10^{-4} \text{ kg.m}^2$$

$$T = I_{\text{total}} \alpha = (0.1973 + 0.0006627) 0.75 = 0.1485 \text{ N.m}$$

### Appendix 3

**Gantt Chart**

No	Detail/Week	1	2	3	4	5	6	7	8	9	10	11	12	13	14	15
1	Project Work Continues															
	1.1 Design and Analysis with Autodesk Inventor and ANSYS Software															
2	Submission of Progress Report															
3	Project Work Continues															
	3.1 Validate design and simulation															
4	Pre-EDX															
5	Submission of Draft Report															
6	Submission of Dissertation (soft bound)															
7	Submission of Technical Paper															
8	Oral Presentation															
9	Submission of Project Dissertation (Hard Bound)															

 Mid semester break